Investigating the role of TWINS protein in regulating seasonal physiology in *Drosophila melanogaster*

By

HAYLEY SHEEHY

THESIS

Submitted in partial satisfaction of the requirements for the degree of

MASTER OF SCIENCE

in

Integrative Genetics and Genomics

in the

OFFICE OF GRADUATE STUDIES

of the

UNIVERSITY OF CALIFORNIA

DAVIS

Approved:

_____

Joanna Chiu, Chair

_____

David Begun

_____

Susan Lott

Committee in Charge

2022

Abstract

Seasonal changes in temperature and photoperiod necessitate a wide range of organisms to adjust their physiology and behavior to survive an unfavorable environment. In insects, one of the main seasonal adaptations is reproductive dormancy. It is the complete arrest of reproductive output and typically occurs in winter. In a previous study, our lab found that EYES ABSENT (EYA) was involved in promoting reproductive dormancy, but the molecular mechanism underlying its role in seasonal regulation is poorly understood. Because EYA has been shown to regulate Protein Phosphatase 2A (PP2A) through binding to the B55a/TWINS (TWS) subunit, we proposed a coincidence model that suggests the interaction between EYA and TWS may promote winter physiology by dephosphorylating substrates in the insulin signaling pathway. The insulin signaling pathway is known to promote summer physiology when activated by phosphorylation. Although previous reports showed that EYA protein cycles over the 24 hours (h) with peak protein expression shifting from day to nighttime in laboratory simulated summer and winter conditions respectively, I observed that summer and winter EYA expression in a fly strain expressing a TWS-GFP fusion protein vs in a wild type strain were inconsistent. Because GFP tags can alter protein function and protein-protein interactions, I constructed a TWS antigen to generate a TWS polyclonal antibody for detecting endogenous levels of TWS protein, which will allow future experiments to assay TWS expression and function without a protein tag and enable investigation of the role of TWS in seasonal physiology.

Introduction

Seasonal differences in day length (also known as photoperiod) and temperature at temperate latitudes necessitate organisms to adjust their physiology and behavior to survive non-optimal environmental conditions. These adaptations allow organisms to take advantage of available resources when they are plentiful and reduce energy demand when resources are depleted. Animals display a variety of strategies to maximize their survival and reproductive output in response to changes in photoperiod and temperature, including migration, altered metabolism, and seasonal reproduction.

Migration is a widely used behavioral strategy that allows animals to move from a geographical area with fewer resources to one with more favorable conditions (e.g., food availability and reproduction) and has evolved in multiple species from insects to vertebrates. Travel lengths can range from relatively short distances to across different continents or hemispheres. One of the best-known migratory insects is the monarch butterfly (*Danaus plexippus*), which can travel up to 4500 km (Flockhart et al., 2017) and requires multiple generations to reach their overwintering site in Mexico from their northern breeding grounds in eastern North America and Canada (Flockhart et al., 2013; Merlin et al., 2020; Reppert & de Roode, 2018). In addition, the dragonfly, *Pantala flavescens*, migrates seasonally, arriving in Middle Asia during the spring and migrating south to East Africa during the fall either through a direct route or a more circular route through India and crossing over the Indian Ocean for a trip that can take up to 14,000 km (Borisov et al., 2020). In birds, previous studies have shown an increase in activity at night during the migratory periods in spring and fall for the redheaded

bunting (*Emberiza bruniceps*) (Sharma et al., 2022) and the garden warbler (*Sylvia borin*) (Gwinner, 1996), which is the result of an endogenous circannual clock.

Changes in photoperiod and temperature can modulate hormone levels throughout the year, which result in precise timing of different metabolic states for a wide range of taxa. With the lower temperatures and reduced amount of food available during the winter, animals will enter a hypometabolic state, such as hibernation or torpor, to conserve energy until spring. The main distinguishing trait between hibernation and torpor is hibernators greatly reduce their metabolic rate and body temperature for several consecutive days at a time, whereas this phenomenon will occur for only a few hours each day in animals that utilize daily torpor (Ruf & Geiser, 2015). In mammals, it has been shown that the photoperiodic control of melatonin and thyroid hormone levels can induce torpor. Thyroxine (T4) levels were higher and triiodothyronine (T3) levels were lower in fall and winter during torpor season for Djungarian hamsters (*Phodopus sungorus*) (Seidel et al., 1987). When the amount of available T3 was increased in hamsters exposed to short photoperiod, this increase in T3 prevented hamsters from experiencing torpor bouts (Murphy et al., 2012). In arctic ground squirrels (*Urocitellus parryii*), warmer temperatures during hibernation causes increased thyroid hormone signaling and hibernation termination (Chmura et al., 2022).

Seasonal changes in photoperiod and temperature can also regulate reproductive output in mammals, birds, and invertebrates. For example, the hypothalamo-pituitary-gonad (HPG) axis in birds is activated or deactivated in response to photoperiod and can change gonad size by 100-fold between the breeding and non-breeding seasons (Dawson et al., 2001). The golden hamster (*Mesocricetus auratus*) is a long-day breeder, where males require at least 12.5

hours of daylight to retain gonadal function (Hong & Stetson, 1986). Because sheep are short-day breeders, photoperiod has the opposite effect compared to the golden hamster and other long-day breeders; ewes exposed to short days were reproductively active with the onset of the breeding season, whereas ewes exposed to long days were reproductively inactive (Legan & Winans, 1981).

For insects, one of the most well-documented seasonal responses is diapause, which affects development and reproduction. For example, pitcher-plant mosquito larvae (*Wyeomyia smithii*) arrest development in short photoperiod (Bradshaw & Phillips, 1979). In addition to pitcher-plant mosquito larvae, insects can initiate diapause in other developmental stages, such as embryos (the commercial silkmoth, *Bombyx mori*), pupae (flesh fly, *Sarcophaga crassipalpis*) and adults (mosquito, *Culex pipiens*) (Sim & Denlinger, 2013).

In my thesis, I will be focusing on seasonal physiology of insects, particularly diapause (or reproductive dormancy) in *Drosophila melanogaster*. Unlike other insect species, *Drosophila melanogaster* requires both short days and cold temperature (~10°C) to enter reproductive dormancy (Saunders & Gilbert, 1990), which caused doubt over whether this species is an appropriate model for diapause; however, several studies have shown that photoperiod may play a larger role in reproductive dormancy (Abrieux et al., 2020; Anduaga et al., 2018; Nagy et al., 2018). Given its versatile genetic tools to manipulate relevant molecular pathways, I decided to use *Drosophila melanogaster* as a model for investigating the genetic mechanisms underlying seasonal physiology.

Chapter 1: Characterizing the mRNA and protein expression pattern of TWINS in laboratory-simulated summer and winter conditions

Introduction

EYES ABSENT (EYA) – which is first characterized in insects and is involved in eye development (Bonini et al., 1993) – is a conserved protein present in birds (e.g., Japanese quail, Nakao et al., 2008) and mammals (e.g., Soay sheep, Dupré et al., 2010). EYA has been found to be upregulated in the pituitary glands in response to the shift from short photoperiod into long photoperiod conditions (Nakao et al., 2008; Dupré et al., 2010), and has also been reported to regulate seasonal adaptations in the fruit fly, *Drosophila melanogaster*. In insects, one of the main seasonal adaptations is the complete arrest in reproductive output, also known as reproductive dormancy. Ovary size is used as a readout for studying seasonal adaptation, where ovaries are larger in summer and smaller in winter (Figure 1.1). The Chiu lab has previously shown that EYA plays a role in promoting reproductive dormancy in laboratory-simulated winter condition (Abrieux et al., 2020). When EYA is overexpressed, the ovaries in long photoperiod shrink and resemble those found in short photoperiod conditions (Abrieux et al., 2020). When EYA expression is reduced, the exact opposite effect occurs, and ovary size remains large during both long and short photoperiod conditions (Abrieux et al., 2020). The mechanism for how EYA induces reproductive dormancy is unknown. In previous studies, the insulin signaling pathway, which is highly regulated by phosphorylation, has been shown to regulate seasonal adaptation (Ojima et al., 2018). When insulin signaling is turned on, it results in mature ovaries; however, impaired insulin signaling increases incidence of reproductive

dormancy (Denlinger, 2022; Sim & Denlinger, 2013). Phosphatase 2A (PP2A) and its B55a/TWINS (TWS) regulatory subunit have been shown to dephosphorylate mitotic kinases (Mayer-Jaekel et al., 1994) and promote mitotic exit (Larouche et al., 2021). Given EYA regulates PP2A through binding to the TWS regulatory subunit (Zhang et al., 2018) in the process of tumorigenesis, I hypothesize that EYA regulates PP2A through binding to TWS and induces reproductive dormancy by inhibiting the insulin signaling pathway.

TWS protein expression peaks during the evening (Wang et al., 2020), and daily rhythmicity of EYA protein expression changes between summer and winter conditions (Abrieux et al., 2020). We hypothesize that because EYA expression peaks during the evening only in the winter, TWS and EYA expression only correspond during this time in winter. As a result, we proposed a coincidence model to illustrate the role of EYA in reproductive dormancy (Figure 1.2). In the summer, EYA peak expression is during the day, while TWS peak expression is at night. Because EYA protein expression is lower at night, there is a lower probability that EYA will bind to the TWS subunit, which leaves PP2A inactive and the insulin signaling pathway activated, resulting in mature ovaries. In the winter, EYA and TWS both have peak expression during the night, so it is more likely they will interact and the role of EYA as a regulator of PP2A is activated. This activation allows PP2A to dephosphorylate key proteins in the insulin signaling pathway, which inhibits insulin signaling and induces reproductive dormancy.

This chapter will describe experiments to assay *tws* mRNA and TWS protein expression in laboratory simulated summer and winter conditions as previous published reports only tested expression of *tws*/TWS in 25°C and 12 hours: 12 hours Light:Dark (12:12 LD) photoperiod.

Materials and Methods

Fly Stocks

Wild type (w^{1118}) *Drosophila melanogaster* was used to assay mRNA expression of *tws*, *eya*, and *per* in summer and winter conditions. Due to the lack of an available TWS antibody at the initial phase of the project, flies expressing *GFP-FLAG-TWS* fusion protein (BDSC no. 63194) were used for assaying TWS protein expression. All fly stocks were raised on Bloomington media at room temperature.

Steady state mRNA expression analysis using quantitative RT-PCR

w^{1118} flies were entrained for 3 days in either 8:16 LD at 10°C or 16:8 LD at 25°C and collected on dry ice every 4 hours on the fourth day. Fly head separation, RNA extraction, quantitative RT-PCR (qRT-PCR) protocol, and data analysis methods were described in Abrieux et al., (2020). Two technical replicates were performed for each of the five biological replicates. Superscript IV (Life Technologies) was used to generate cDNA and SsoAdvanced Universal SYBR Green Mix (Biorad) was used to perform quantitative PCR reactions. The primer sequences to amplify each gene were: *tws* forward, 5'-CCAAGCTGTGCTCGCTGTACG-3'; *tws* reverse, 5'-GCCGCCAGTGCAAACTTTCCGT-3'; *eya* forward, 5'-GCTTTGGGCGCAAGAGCACCT-3'; *eya* reverse, 5'-GAGGGCGCGAATGTCGCTGT-3'; *per* forward, 5'-GACCGAATCCCTGCTCAA-3'; *per* reverse, 5'-GTGTCATTGGCGGACTTC-3'; *cbp20* forward, 5'-GTCTGATTCGTGTGGACTGG-3'; *cbp20* reverse, 5'-CAACAGTTTGCCATAACCCC-3'. The qPCR reaction conditions were 30 seconds at 95°C, 40 cycles of 5 seconds at 95°C and an annealing/extension stage of 30 seconds at 60°C. A melt

curve analysis concluded the reaction with 0.5°C stepwise increments starting at 65°C and finishing at 95°C. Because *cbp20* mRNA expression remained unchanged regardless of photoperiod and temperature, it was used as the reference gene to normalize for RNA input and assay changes in target genes (*eya* and *tws*). *per* was used as a positive control due to its rhythmic mRNA expression pattern in all photoperiod and temperature conditions used in the experiments. Data were analyzed using the $\Delta\Delta$CT method and Ct values for all timepoints were scaled to be between 0 and 1 by dividing all values by the highest Ct value to compare relative mRNA expression.

Protein expression analysis using Western blots

Because no TWS antibody is commercially available at the beginning of this project, I used the *GFP-FLAG-TWS* (BDSC no. 63194) fly strain, which expresses GFP-tagged TWS as a fusion protein. Detection of GFP was used as an indirect way of measuring TWS protein expression. Flies were entrained in 8:16 LD at 10°C or 16:8 LD at 25°C for three days and collected on dry ice every four hours on the fourth day. Fly head separation, protein extraction, and western blotting were performed as described in Abrieux et al. (2020). Antibodies were incubated in 5% blocking reagent (Bio-Rad) diluted in 1X TBST. Primary antibodies were diluted as the following: mouse α-EYA (eya10H6, DSHB) at 1:1000, rabbit α-GFP (gift from Dr. Bo Liu, UC Davis) at 1:10000, and mouse α-HSP70 (Sigma) at 1:10000. Secondary antibodies were diluted as the following: mouse α-IgG (Cytiva Life Sciences) at 1:1000 for detecting α-EYA and at 1:10000 for detecting α-HSP70, and rabbit α-IgG (Cytiva Life Sciences) at 1:10000 for detecting α-GFP. Blots were imaged using the ChemiDoc MP system and Image Lab software

(version 5.0 build 18) (BioRad). Protein was quantified and normalized to Ponceau (Sigma) total protein staining using the Image Lab software.

Co-immunoprecipitation (CoIP) in Drosophila *S2 cells*

Using Effectene Transfection Reagent (Qiagen) according to the manufacturer's protocol, 3 x 10^6 S2 cells were transiently transfected with each of the following combinations of plasmids: 1) pAc-*tws*-V5 and pAct-*eya*-3XFLAG-6XHIS, 2) pAc-*tws*-V5 and pAc 5.1B-3XFLAG-6XHIS, and 3) pAct-*eya*-3XFLAG-6XHIS and pAc-V5-HIS. Cell harvest and protein extraction: Cells were centrifuged at 4000 rpm for 4 minutes at 4°C, then washed with 1X PBS and resuspended in 2 mL of modified RIPA buffer (Stock solution: 50 mM Tris-HCL pH7.5, 150 mM NaCl, 1% NP40, 0.25% Na-deoxycholate; added to stock solution immediately before performing protein extraction: 1 mM EDTA, 25 mM NaF, 0.5 mM PMSF, and 1X complete EDTA-free protease inhibitor mixture). Lysates were centrifuged at high speed at 4°C and supernatant was collected as input protein for IP. Immunoprecipitation: Samples were pre-cleared with gammabind sepharose to reduce non-specific binding. Prior to use, the beads were washed with 1X TBS and equilibrated with modified RIPA buffer. The same volume of settled beads were used for each IP. Protein extracts were quantified with Coomassie Plus – The Better Bradford Assay Reagent (ThermoFisher Scientific) and concentration was measured on the BioRad Spectrophotometer at 595nm. Equal amount of protein extracts from each sample was added to tubes with beads conjugated with either α-V5 or α-FLAG antibodies for IP. Samples were incubated for 4 hours at 4°C using end-over-end rotator, and non-specific binding was minimized by subsequently washing 3 times with modified RIPA buffer. At the conclusion of the

last wash, 2X SDS sample buffer was added to each IP sample. Samples were boiled at 95°C for 5 mins prior to resolving on SDS-PAGE gel. The primary antibodies α-V5 (1:5000) and α-FLAG (1:7000) with secondary antibody α-mouse IgG (1:2000) were used for protein visualization.

Statistical Analysis

Cycling statistics (rhythmicity, peak, peak.shape, period) of mRNA and protein expression were calculated using the RAIN package in R (Thaben & Westermark, 2014). Other statistical analyses were performed in GraphPad Prism 9.0 (GraphPad Software, USA) using similar protocols from Abrieux et al. (2020). In brief, two-way ANOVA with Tukey's multiple comparisons tests were performed to analyze differences in mRNA and protein expression between each timepoint and condition. Error bars are the standard error of the mean (SEM). Statistical significance is indicated using asterisks for differences between conditions for each timepoint.

Results

tws *and* eya *mRNA exhibit rhythmic expression that varies with seasonal conditions*

From the coincidence model (Figure 1.2), one assumption that I have is the daily rhythm of TWS protein expression does not change in response to photoperiod and TWS expression will peak in the dark phase in both simulated summer and winter. I hypothesize that because EYA protein expression peaks during the evening only in the winter, TWS and EYA protein expression only correspond in winter, thus promoting winter physiology. In addition to testing this hypothesis by assaying TWS and EYA expression, I wanted to determine if the same

expression pattern is true at the mRNA level. I therefore entrained wild type w^{1118} flies for three full days in either summer (16L:8D at 25°C) or winter (8L:16D at 10°C) conditions and collected fly samples every four hours over a 24-hour period on the fourth day for quantitative RT-PCR analysis. Daily mRNA expression of *eya* and *tws* were measured by qPCR and normalized using the housekeeping gene, *cbp20*, which has stable mRNA expression regardless of temperature, photoperiod, or time of day (Figure 1.3). *tws* mRNA expression was observed to be rhythmic over the 24-hour cycle in winter (p-value = 0.034; peak = ZT12; RAIN), but not in simulated summer conditions (p-value = 0.85; RAIN) (Figure 1.3A). It is also shown that time points ZT 4, 8 and 12 have significantly higher *tws* mRNA expression in winter compared to summer (Figure 1.3A, p-value <0.05, Two-way ANOVA with Tukey's multiple comparisons test). Time points ZT 16 and 20 also trend toward higher *tws* mRNA expression in winter than summer conditions, but the difference is not statistically significant. The difference in *eya* mRNA expression between these seasonal conditions follows a similar pattern. The time points ZT 4, 8, and 20 have significantly higher mRNA expression in winter compared to summer (Figure 1.3B, p-value <0.05, Two-way ANOVA with Tukey's multiple comparisons test). The other three time points (ZT 12, 16, 24) all seem to have higher mRNA expression in winter, but the differences were not statistically significant. In contrast to *tws*, *eya* mRNA expression has the opposite pattern, where *eya* exhibits daily rhythmic expression in summer (p-value = 0.041; peak = ZT16; RAIN), but not in winter conditions (p-value = 0.94; RAIN) (Figure 1.3B). I also measured mRNA expression pattern of *per* as a rhythmic, positive control gene for our analysis, and it was shown to have daily rhythmic mRNA expression in both summer and winter (summer: p-value = 1.60E-08; peak = ZT16; winter: p-value = 2.64E-05; peak = ZT12; RAIN). All time points, except ZT 24,

exhibit higher *per* mRNA expression in winter than summer (Figure 1.3C, p-value <0.05, Two-way ANOVA with Tukey's multiple comparisons test).

GFP-TWS protein expression is rhythmic in summer conditions and peaks at ZT 8

After measuring the mRNA, I measured daily EYA and TWS protein expression patterns in summer and winter. Because I did not have a TWS antibody at the time, I used the *GFP-FLAG-TWS* fly strain, which produces TWS as a fusion protein tagged with GFP allowing me to detect GFP to indirectly measure TWS expression level. GFP-TWS protein exhibits daily rhythmic expression in summer conditions and peaks at ZT 8 but is not rhythmic in winter (Summer: p-value = 0.00038; Peak = ZT8; Winter: p-value = 0.29; RAIN). The differences in mRNA expression between conditions for each time point is not statistically significant (Figure 1.4A, p-value >0.05, Two-way ANOVA with Tukey's multiple comparisons test).

To correlate TWS and EYA expression, I also measured EYA protein expression in the same *GFP-FLAG-TWS* flies. Surprisingly, EYA is not rhythmic in either simulated summer or winter conditions (summer: p-value = 0.51; winter = 0.74; RAIN), and there is no significant difference between conditions for each time point (Figure 1.4B, p-value >0.05, Two-way ANOVA with Tukey's multiple comparisons test). These results were not consistent with my qPCR data nor our previously published results, where EYA protein expression was rhythmic in winter and peaked at ZT 16 (Abrieux et al., 2020).

EYA protein expression is rhythmic in summer and peaks at ZT 20 in w^{1118} *flies*

Because EYA protein expression in *GFP-FLAG-TWS* flies were not consistent with previously published results, I evaluated w^{1118} flies in simulated summer and winter conditions to confirm EYA protein expression is cycling in wild type flies rather than using *GFP-FLAG-TWS* flies. Wild type w^{1118} flies were kept in 12:12 LD at 25°C for three days then moved to either summer or winter conditions for seven days. Flies were collected every four hours over a 24-hour period on the seventh day and head extracts were used for Western blot analysis. Interestingly, EYA protein expression in w^{1118} flies follows a similar pattern as the mRNA expression in w^{1118} flies, where EYA has rhythmic expression in summer with a peak at ZT 20 (p-value: = 0.019; Peak: ZT20; RAIN) and is arhythmic in winter (p-value: 0.72; RAIN) (Figure 1.5). This pattern contrasts with the EYA protein expression pattern in *GFP-FLAG-TWS* flies, where EYA was arhythmic in both summer and winter (Figure 1.4).

EYA and TWS physically interact in S2 cells

Based on our coincidence model, I also hypothesized that EYA and TWS preferentially interact in winter conditions when peak expression for both proteins overlap and have the greatest probability of physical interaction (Figure 1.2). To test this hypothesis, I first determined if EYA and TWS proteins interact in *Drosophila* cells by performing coimmunoprecipitation (coIP) in *Drosophila* S2 tissue culture. S2 cells were transfected with either EYA-FLAG + empty vector, TWS-V5 + empty vector, or EYA-FLAG + TWS-V5. Upon cell harvest, protein extracts were immunoprecipitated with either α-V5 or α-FLAG. When the IP-FLAG reactions were detected with α-V5 for Western blot analysis, there were faint bands

detected in all the IP-FLAG reactions, which indicate non-specific binding (Figure 1.6). However, when using α-FLAG to detect for the presence of EYA in the reciprocal α-V5 coIP reactions, I see that EYA-FLAG is successfully detected in IP with α-V5, which indicates that EYA and TWS physically interact in the S2 cells (Figure 1.6).

Discussion

In previously published results from our lab, we found that *eya* plays a role in inducing reproductive dormancy in *Drosophila melanogaster* (Abrieux et al., 2020); however, the mechanism for how *eya* is involved in this process is unknown. To answer this question, our lab proposed a coincidence model for a possible mechanism of the role of *eya* in reproductive dormancy (Figure 1.2). In the coincidence model, I hypothesized that peak EYA protein expression is during the day in summer and during the night in winter, while peak TWS protein expression occurs at night regardless of season (Figure 1.2).

My observations from this study exhibited mixed results regarding the model. I showed *tws* mRNA expression is rhythmic in winter and peaks at night at ZT 12 in wildtype w^{1118} flies, which supports our model; however, *tws* mRNA expression is not rhythmic in summer and does not agree with our model (Figure 1.3A). Also, *eya* mRNA expression had an opposite pattern compared to *tws* with rhythmic mRNA expression in summer peaking at ZT 16 and arhythmic mRNA expression in winter (Figure1.3B). Even though the rhythmicity of *tws* and *eya* mRNA expression in summer and winter may not match the expectations from the coincidence model, both genes have higher mRNA expression during winter – with a few time points having significantly higher mRNA expression, compared to summer – which can indicate a higher

probability for proteins encoded by *eya* and *tws* to interact during winter and induce reproductive dormancy (Figures 1.2, 1.3A and B). However, the model predicted these interactions to occur at the protein level in summer and winter conditions.

To evaluate my hypothesis that peak EYA and TWS protein expression coincide in winter and not summer, I assayed daily TWS and EYA expression in GFP-tagged *GFP-FLAG-TWS* flies (due to no TWS antibody available) in summer and winter conditions. I observed rhythmic protein expression of GFP-TWS peaking at ZT 8 in summer, but arhythmic protein expression in winter, which contrasts with the *tws* mRNA expression pattern I observed.

For EYA, I observed that there was no rhythmicity or any significant differences in protein expression between summer and winter conditions for any of the timepoints in *GFP-FLAG-TWS*. As a result, I was not able to replicate previously published results (Abrieux et al., 2020) using the *GFP-FLAG-TWS* flies. Because these observations may be a consequence of the GFP-tagged fusion TWS protein, I subsequently measured EYA protein expression in wild type w^{1118} flies for comparison. I found that EYA protein expression was rhythmic in summer with peak expression at ZT 20 and arhythmic in winter (Figure 1.5). Compared to the *eya* mRNA expression, the peak expression in EYA was delayed by four hours, but had similar expression patterns overall in w^{1118}, which leads me to think the GFP tag may have been problematic for this study. Nevertheless, it is still surprising that daily EYA expression is not rhythmic in simulated winter conditions, as previously shown in Abrieux et al. (2020).

Previous studies have shown that large tags, such as GFP and mCherry, can disrupt protein function and protein-protein interactions. For example, the protein, spastin, plays an important role in microtubule severing (Kuo et al., 2019; Solowska et al., 2014), and loss-of-

function mutations in this protein causes a disease called hereditary spastic paraplegia in humans (Akaba et al., 2021; Giordani et al., 2021; Varghaei et al., 2022). When investigating the degradation of spastin via ubiquitination, researchers found that when ubiquitin is tagged with GFP or mCherry and overexpressed in mammalian cell culture, ubiquitin does not degrade spastin; however, when ubiquitin is tagged with a smaller tag, such as FLAG, ubiquitin functions normally and results in the degradation of spastin (Zou et al., 2021). When the molecular motor, kinesin-1, is tagged with a fluorescent tag in mammalian cell culture, the motor can run longer lengths than normal (Norris et al., 2015). In bacteria, previous studies have shown that fluorescent tags, such as GFP, impair the function of the bacterial flagellar motor (Heo et al., 2017; Morimoto et al., 2020). Fluorescent-labeled proteins have also been shown to affect the function of the original protein in viruses (Costantini & Snapp, 2015) and bacteria (Margolin, 2012; Swulius & Jensen, 2012) as well as cause dilated cardiomyopathy in transgenic mice (Huang et al., 2000). These studies show how large fluorescent tags, such as GFP, can alter protein function in a wide variety of organisms, which leads me to reevaluate my strategy for investigating the possible connection between EYA and TWS in reproductive dormancy.

Because I observed EYA and TWS physically interact in S2 cells (Figure 1.6) and the possible effect of GFP-tagged TWS on TWS protein function and binding capability, I decided to produce a TWS antibody that can be used to detect endogenous TWS expression in wild type flies. This antibody will also facilitate the simultaneous examination of EYA and TWS expression in the same flies in response to changes in seasonal conditions. Finally, the generation of a TWS antibody will open more avenues to investigate the potential interaction between EYA and TWS *in vivo*.

Chapter 2: Generating and Validating a polyclonal antibody for *Drosophila* TWINS protein

Introduction

As an integral part of the adaptive immune system, B cells produce antibodies to target and combat viruses and other pathogens. Antibodies are made into a variety of forms with unique sequences of amino acids and antigen-binding sites and are one of the most abundant protein components in the blood (Alberts et al., 2002). When a B cell first produces an antibody, it resides on the outside surface of the plasma membrane and acts as an antigen receptor. Only one type of antibody is produced by each B cell, and when it binds to an antigen, the B cell differentiates into effector cells that produce large amounts of soluble antibodies for secretion (Alberts et al., 2002). As a result of this antibody production process performed by the immune system, researchers have taken advantage of the antibodies' ability to recognize specific proteins and use them to answer questions in basic research as well as play an important role in diagnostics and therapeutics in the biotechnology and pharmaceutical industries (Kennedy et al., 2018).

Conventional antibodies come in two different forms: polyclonal and monoclonal. Polyclonal antibodies come from antibody-producing plasma cells derived from multiple B cell clones (Howard & Kaser, 2013). Several weeks after an animal is injected with the antigen of interest, the serum containing the polyclonal antibody is collected (Peltomaa et al., 2022). Multiple immunizations can help maximize the immune response against the antigen and decrease any non-specific binding (Howard & Kaser, 2013). Commonly used animals include mice, rats, rabbits, guinea pigs and hamsters as well as larger animals such as sheep and goats

(Peltomaa et al., 2022). Polyclonal antibodies have been used for identifying antigens for applications including western blots, radioimmunoassay, enzyme-linked immunosorbent assays, indirect and direct fluorescent antibody test, hemagglutination tests, immunohistochemistry, immunoprecipitation assays, immunodiffusion, affinity chromatography, enzymology, and isolation of gene products (Howard & Kaser, 2013). Polyclonal antibodies are relatively inexpensive and quick and easy to produce with high overall affinity against their target compared to other methods of generating antibodies (Peltomaa et al., 2022). On the other hand, polyclonal antibodies have shown to have several limitations. Because they derive from a mixture of different B cell clones, each batch of polyclonal antibodies will not be identical, which leads to reproducibility issues and variable sensitivity to the target antigen (Peltomaa et al., 2022). These issues are resolved with the production of monoclonal antibodies.

With the development of hybridoma technology, the production and commercialization of monoclonal antibodies have opened the door for new therapeutics to enter the market (Eaglesham et al., 2021; Ecker et al., 2015; Galfrè & Milstein, 1981; Köhler & Milstein, 1975). Hybridomas were first produced in mice and later introduced to rabbits, resulting in monoclonals possessing higher affinities to their targets (Kennedy et al., 2018). Similar to polyclonal antibodies, monoclonal antibodies are developed by immunizing animals – such as mouse, rat or hamster – with the target antigen to produce antigen-specific B cells (Peltomaa et al., 2022). These B cells are then fused with myeloma cells creating hybridomas, which are then cloned and tested for antigen specificity (Peltomaa et al., 2022). Monoclonal antibodies can produce large amounts of identical antibodies and reduce variation between batches, which

puts them at an advantage over polyclonal antibodies (Peltomaa et al., 2022). Because of this advantage, monoclonal antibodies have been developed and commercialized as therapeutics for various diseases. As of 2021, a total of 131 antibody therapeutics have been approved for the treatment of cancer, immune-mediated disorders, infectious diseases, cardiovascular/hemostasis, neurological disorders, genetic diseases, ophthalmic disorders, and musculoskeletal disorders (Kaplon et al., 2022). Despite its advantages over polyclonal antibodies and the successful therapeutic applications in the pharmaceutical industry, monoclonal antibodies have significant downsides that need to be resolved. For example, they are not as specific as one would expect and have shown to bind off-target (Bradbury et al., 2018). This non-specific binding can be due to cross-reactivity with similar epitopes or the production of additional antibody chains during hybridoma generation (Bradbury et al., 2018). In addition to these deficiencies, changes in the epitope structure due to genetic polymorphism, glycosylation or denaturation as well as any changes in pH or salt concentration can negatively impact antibody function, and these types of antibodies are very expensive and time-consuming to produce (Lipman et al., 2005).

Due to the inconsistent results of using anti-GFP antibody to detect GFP-tagged TWS protein expression patterns in summer and winter conditions as described in the previous chapter and the possibility that GFP fusion could disrupt endogenous TWS expression and function, I deemed it necessary to produce an antibody that directly measures TWS for more accurate results. Because they are relatively inexpensive and easier to make, I decided to produce a polyclonal TWS antibody to set the stage for better understanding the expression of

TWS in different seasonal conditions, the physical interaction between EYA and TWS, as well as the role of TWS in reproductive dormancy.

Materials and Methods

TWS expression construct design

Using the AlphaFold protein structure database to exclude disordered portions of the TWS polypeptide (Jumper et al., 2021; Varadi et al., 2022), three portions of the TWS protein were chosen for antigen production: amino acids 61 through 222 [TWS(61-222aa)], amino acids 231-392 [TWS(231-392aa)], and amino acids 61 through 392 [TWS(61-392aa)]. Primers were designed to amplify these cDNAs by PCR and a stop codon is added at the end of the predicted protein. The resulting PCR products and pHis (pET22b) expression vector (gift from Dr. Carrie Partch, UC Santa Cruz) were digested with NotI and NcoI restriction enzymes, and the resulting fragments were ligated together. The resultant constructs – pHis-TWS(61-222aa), pHis-TWS(231-392aa), and pHis-TWS(61-392aa) – were transformed in *E. coli* DH5α and the construct sequences were confirmed via Sanger sequencing. The primers for each construct were the following: TWS(61-222aa) Forward, 5'-GTGTCCATGGATAATCCGAGACGCGGCGAATACAAT-3', Reverse, 5'-GTGTGCGGCCGCCTATAGCTCCTCCATGTTGGTTGGCTT-3'; TWS(231-392aa) Forward, 5'-GTGTCCATGGATCATCCGACCGAGTGCAATGTGT-3'; Reverse, 5'-GTGTGCGGCCGCCTACCGTGGCTTAAGCACCGTTTTC-3'; TWS(61-392aa) Forward, 5'-GTGTCCATGGATAATCCGAGACGCGGCGAATACAAT-3'; Reverse, 5'-

GTGTGCGGCCGCCTACCGTGGCTTAAGCACCGTTTTC-3'. Plasmid DNA was extracted using the PureLink Quick Plasmid Miniprep Kit (Invitrogen).

Expression of N-terminal His-tagged TWS recombinant protein

5 uL of each plasmid miniprep DNA was transformed into the BL21 *E. coli* strain and grown on LB-Amp plates overnight. Individual colonies were selected and subsequently cultured in 25 mL LB broth with 125 ug/mL ampicillin overnight at 37°C, 225rpm. The next morning, 500mL LB broth with 125ug/mL ampicillin was inoculated with 5 mL of the overnight culture and grown at 30°C, 225rpm until A_{600} was around 0.6. The bacterial culture was incubated at 4°C for 45 minutes to stop bacterial growth. After incubation, 250uL aliquot of the culture was taken out [IPTG (-) sample]. The culture was induced with 1mM isopropyl-B-d-thiogalactopyranoside (IPTG) and grown overnight at 18°C, 225rpm. The next morning, 250 uL aliquot of induced culture was taken out [IPTG (+) sample]. Both IPTG (-) and IPTG (+) samples were centrifuged at 4000 rpm at 4°C for 1 minute and supernatants were removed. Each pellet was resuspended in 30 uL of 2X SDS sample buffer and stored in -20°C. The rest of the induced culture was centrifuged at 5000 rpm at 4°C for 15 minutes and the pellet was resuspended in 40 mL modified TEV buffer (50mM $NaPO_4$, 300mM NaCl, 10% glycerol, 0.1% Triton X-100, 20mM imidazole, 5mM beta-mercaptoethanol). Cells were lysed using a microfluidizer and lysed cells were split into two 50-mL falcon tubes with the addition of 10uL DNase I. Both tubes of lysed cells were incubated at 4°C on a nutator for 1 hour. After DNase I treatment, the two tubes of lysed cells were combined and 100uL aliquots were removed for testing expression and solubility of each construct. The aliquots were centrifuged at 14000 rpm at 4°C for 15

minutes. The supernatant was transferred to a new 1.5mL microcentrifuge tube and 100uL 2X SDS sample buffer was added to both the supernatant (soluble portion) and the pellet (insoluble portion). The rest of the lysed cells were centrifuged at 13000 rpm at 4°C for 30 minutes, and the supernatant was removed. The pellet was resuspended in 5mL of 50mM $NaPO_4$ + 1% sodium dodecyl sulfate (SDS) and heated at 95°C, mixing periodically until the pellet is fully resuspended. The resuspended pellet was diluted in denaturing sample buffer, so the final concentrations were 50mM $NaPO_4$, 300mM NaCl, 10% glycerol, 0.1% Triton X-100, 5mM imidazole and 0.05% SDS.

TWS antigen purification

In a 4°C cold room, the diluted lysed cell resuspension was passed through a BioRad standard econocolumn loaded with Ni-NTA agarose beads (Qiagen) that was pre-conditioned with 25mL equilibrium buffer (50mM $NaPO_4$, 300mM NaCl, 10% glycerol, 0.1% Triton X-100, 5mM imidazole and 0.05% SDS). The column was washed with 50mL wash buffer (50mM $NaPO_4$, 300mM NaCl, 10% glycerol, 0.1% Triton X-100, 10mM imidazole and 0.05% SDS), and then washed with 20mL elution buffer (50mM $NaPO_4$, 300mM NaCl, 10% glycerol, 0.1% Triton X-100, 200mM imidazole and 0.05% SDS). The eluted pHis-TWS(231-392aa) protein was collected and concentrated to a volume ~5.5mL. Dialysis of pHis-TWS(231-392aa) was performed using the Slide-A-Lyzer™ Dialysis Cassette Kit (ThermoFisher) in 2L of buffer containing 50mM $NaPO_4$, 300mM NaCl, and 10% glycerol and incubated at 4°C overnight. The purity of pHis-TWS(231-392aa) was confirmed via SDS-PAGE and was quantified using Bradford assay (ThermoFisher).

Polyclonal Antibody Production

Two male Wistar rats weighing 250-300g and aged 56-90 days old were immunized to produce TWS polyclonal antibodies. The first immunization was performed using 250ug of pHis-TWS(231-392aa) emulsified in Freund's Complete Adjuvant (FCA) and was injected subcutaneously in the neck. The next five immunizations were performed using 250ug of pHis-TWS(231-392aa) emulsified in Freund's Incomplete Adjuvant about three weeks apart. Immunization was performed by Covance, Inc.

Polyclonal Antibody Validation in Drosophila *Schneider (S2) Cells*

In a 6-well plate, 3 x 10^6 S2 cells were transiently transfected with 0.8ug pAc-*tws*-V5 using Effectene Transfection Reagent (Qiagen) according to the manufacturer's protocol and another 3 x 10^6 S2 cells were seeded but not transfected (Control). Protein Extraction: Prepare EB2 media (100mM KCl, 5% Glycerol, 20mM Hepes pH 7.5, 5mM EDTA, 1mM DTT, 10ug/mL Aprotinin, 5ug/mL Leupeptin, 1ug/mL Pepstatin A, 0.5mM PMSF, 0.1% Triton X-100, 25mM NaF) and keep on ice. The cells were resuspended in the wells by pipetting up and down until the cells no longer adhere to the plate and were transferred into 1.5mL microcentrifuge tubes. Cells were then centrifuged at 4000rpm for 5 minutes at 4°C and the supernatant was removed. The cell pellet was washed once with 1X PBS and centrifuged at 4000rpm for 2 minutes at 4°C. The supernatant was removed, and each cell pellet was resuspended in EB2 buffer on ice. The lysed cells were centrifuged at 13000rpm for 10 minutes at 4°C and the supernatant was transferred to new 1.5mL microcentrifuge tubes. The protein extracts were quantified with Coomassie Plus – The Better Bradford Assay Reagent (ThermoFisher Scientific) and protein

concentration was measured on the BioRad Spectrophotometer at 595nm. Serum from pre-bleed (negative control), α-V5 (positive control), and serum from test bleed were used in Western blotting to detect TWS in both untransfected S2 cells and S2 cells transfected with pAc-*tws*-V5. The primary antibodies were diluted as follows: pre-bleed (1:1000), α-V5 (1:5000), and test-bleed (1:1000). The secondary antibodies were α-mouse IgG (1:2000) for α-V5 and α-rat IgG (1:1000) for both the pre-bleed and test-bleed.

Polyclonal antibody validation in GFP-FLAG-TWS *and* w^{1118} *flies*

For entrainment and collection of wild type (w^{1118}) flies and flies expressing *GFP-FLAG-TWS* as well methods for protein extractions, refer to Methods in Chapter 1.

Multiple sequence alignment

Amino acid sequence for *Drosophila melanogaster* TWS(231-392aa) was imported into a standard BLASTp search and was used to find similar sequences in the non-redundant sequences database (related *Drosophila* species) or the Model Organisms database (vertebrate species). For the *Drosophila* species, the first ten results were selected and visualized using the NCBI Multiple Sequence Alignment Viewer (version 1.22.0). For the model organisms, the top result for each species were selected and visualized using the NCBI Multiple Sequence Alignment Viewer (version 1.22.0).

Results

Three pHis-TWS constructs were generated to target regions of the proteins that might be soluble

Because globular proteins are highly soluble (Shen, 2019), I used the protein structure prediction program, AlphaFold (Jumper et al., 2021; Varadi et al., 2022), to choose the globular region of TWS to maximize the potential for generating a soluble protein for antigen production. Three portions of the TWS protein were chosen: amino acids 61 through 222 [TWS(61-222aa)], amino acids 231-392 [TWS(231-392aa)], and amino acids 61 through 392 [TWS(61-392aa)] (Figure 2.1A, B, C). Each portion was ligated into the expression vector, pHis, between the NcoI and NotI restriction sites and with the 6XHis tag at the N-terminal end of the protein (Figure 2.1D). Each construct was transformed into the *E. coli* strain, DH5α, for plasmid DNA isolation. To confirm that each portion of TWS was ligated into the pHis vector, each construct was digested with NcoI and NotI and visualized via agarose gel (Figure2.1E). Each construct was ligated correctly into pHis and the sequences were validated using Sanger sequencing to check for any mutations or frameshifts that may have occurred.

pHis-TWS(61-222aa) and pHis-TWS(231-392aa) are expressed but insoluble

Once the sequences for the constructs of each TWS fragment were confirmed, each recombinant protein was tested for expression and solubility (Figure 2.2). Each construct was transformed into the *E. coli* strain, BL21, and the pHis-TWS(61-222aa) and pHis-TWS(231-392aa) recombinant proteins were successfully expressed after induction with IPTG; however, SDS-PAGE gel electrophoresis showed they were both insoluble (Figure 2.2A and B). pHis-

TWS(61-392) failed to express any detectable recombinant protein (Figure 2.2C). Ultimately pHis-TWS(231-392aa) was chosen for large scale expression because it appeared to have slightly higher protein expression compared to pHis-TWS(61-222aa) and purifying insoluble proteins under denaturing conditions using a gravity column has been shown to be successful (Koerber et al., 2007; McGraw et al., 2014).

Successful purification of pHis-TWS(231-392aa) under denaturing conditions

Due to the insolubility of pHis-TWS(231-392aa), the protein was purified using Ni-NTA agarose beads in a gravity column under denaturing conditions (Materials and Methods). SDS-PAGE gel electrophoresis showed pHis-TWS(231-392aa) was successfully eluted from the column and 12.823 mg of protein was collected (Figure 2.3, Table 1). About 50% of pHis-TWS(231-392aa) was not recovered after concentration (Table 1). The concentrated pHis-TWS(231-392aa) was dialyzed into buffer containing 50mM $NaPO_4$, 300mM NaCl, and 10% glycerol. The final concentration of pHis-TWS(231-392aa) was 1106.5 ug/mL for a total of 6.086 mg, which is enough for inoculation in animals to produce the α-TWS antibody.

α-TWS polyclonal antibody successfully validated in Drosophila *S2 cells*

To produce an α-TWS polyclonal antibody, purified pHis-TWS(231-392aa) was injected into two Wistar rats for immunization and plasma was collected after three weeks. This was performed by Covance, Inc. Before inoculation, a plasma sample from each rat was collected (pre-bleed) and used as a negative control sample for the validation tests. These pre-bleed sera allow me to see what non-specific background binding is present in the animal before

immunization with the pHis-TWS(231-392aa) antigen. To determine if α-TWS was able to successfully detect TWS, the antibody was validated using *Drosophila* S2 cells that were transfected with the plasmid, pAc-*tws*-V5 and visualized via western blot (Figure 2.4). Because two rats were inoculated with pHis-TWS(231-392aa), there were two antibodies that needed to be tested. For one of the antibodies, TWS was successfully detected as seen in #7279 (Figure 2.4A), where a band of the same size as the V5-tagged TWS positive control has been detected in the TWS-V5 lane and is absent in the control lane. For this antibody, test bleed #4 shows increased signal and decreased non-specific binding when detecting for TWS compared to the first test bleed (Figure 2.4A). These results show that multiple antigen injections of pHis-TWS(231-392aa) into the animal can increase the signal for the target protein and decrease background noise. For the antibody in animal #7280, a band of the same size as the V5-tagged TWS positive control has been detected in both the TWS-V5 lane and the control lane, which indicates non-specific binding (Figure 2.4B). Another injection of pHis-TWS(231-392aa) may help to further increase signal to background noise ratio.

Antibody validation in wild type Drosophila melanogaster *suggests α-TWS polyclonal antibody can detect TWS proteins in fly heads*

Because the α-TWS polyclonal antibody will ultimately be used to detect TWS protein expression in flies, I need to confirm that the antibody is functional in flies. To determine if the α-TWS antibody successfully detects TWS in flies, I used a fly line expressing TWS tagged with GFP and FLAG. This will allow the use of α-GFP Western blot detection to act as a positive control. Since ZT12 seem to have different TWS protein expression levels in summer and

winter conditions (though not significant) for the *GFP-FLAG-TWS* strain when using α-GFP as the primary antibody, I used proteins extracted from flies collected at ZT12 in summer and winter conditions to test the α-TWS antibody in *GFP-FLAG-TWS* (Figure 2.5). For both antibodies tested, there is a band present that is the same size as the α-GFP positive control and is not present in the pre-bleed, which indicates that the antibodies successfully detect TWS (red arrows, Figure 2.5). The antibody #7279 shows less non-specific binding (Figure 2.5A) and antibody #7280 has increased signal when detecting for TWS after multiple immunizations (Figure 2.5B).

After validating the antibody in *GFP-FLAG-TWS,* I wanted to test α-TWS polyclonal antibodies in wildtype, w^{1118} flies. Flies were entrained for 3 days in 12:12 LD at 25°C then maintained for 7 days in either summer or winter conditions. Samples were collected every four hours for a 24-hour period and protein extracts were visualized using western blots. The *tws* gene produces two TWS proteins with slightly different lengths around 50 kD in size (Sathyanarayanan et al., 2004). When examining the samples in summer and winter conditions, there are two bands that are present around the 50 kD marker length in each sample when normalized with Ponceau S stain for total protein, which are likely to correspond to TWS expression (red arrows, Figure 2.6A). When comparing the quantification of TWS in w^{1118} flies with the quantification of GFP-tagged TWS in *GFP-FLAG-TWS* flies, the overall protein expression patterns for each condition follow similar trends, where there is higher protein expression earlier in the day then drops off at night in summer and more constant protein expression for most of the day with a slight increase between ZT20-24 in winter (Figure 2.6C and D). These trends point to the likelihood that the two bands around 50 kD represent TWS.

Sequence analysis to determine utility of TWS antibody in other species

If the utility of TWS polyclonal antibodies is indeed validated in *Drosophila melanogaster* via the use of fly strains expressing *tws* RNAi and/or overexpressing *tws* in future validation experiments, then it may be interesting to determine if this antibody can be used to detect homologous TWS proteins in other species. To examine this possibility, I used BLASTp to determine if the TWS antigen sequence was conserved in other *Drosophila* species. Figure 2.7A shows the top ten BLASTp search results and found that all, apart from *Scaptodrosophila lebanonensis* at 99.38% Identity, had shown 100% Identity with the *Drosophila melanogaster* TWS antigen sequence and around 80.75% Identity with the homologous TWS protein in mice, humans, and zebrafish (Figure 2.7B), which indicates there is a possibility for the TWS antibody to detect TWS in each of these species (Bolander et al., 1989).

Discussion

Researchers in academia and the pharmaceutical industry have taken advantage of the immune system's ability to produce a wide variety of antibodies for their own research and treatment options, respectively (Kennedy et al., 2018; Eaglesham et al., 2021; Ecker et al., 2015; Galfrè & Milstein, 1981; Köhler & Milstein, 1975). Conventional antibodies are produced in two different forms – polyclonal and monoclonal – each with their own advantages and disadvantages. Even though polyclonal antibodies have more limitations regarding reproducibility, they are much easier, quicker, and less expensive to produce compared to monoclonal antibodies (Peltomaa et al., 2022).

In this study, I produced a polyclonal TWS antibody that directly measures TWS protein expression. In the process of producing an α-TWS antibody, several unsuccessful attempts were made. Following a similar method for producing pHis-TWS(231-392aa), the full-length *tws* ORF was first inserted into the pHis expression vector (based on pET22b from Partch lab, Materials and Methods) between the NotI and NcoI restriction sites and transformed into *E. coli* BL21; however, the pHis-TWS recombinant protein failed to be expressed and could not be purified (Figure 2.8). This could be due to the presence of disordered regions, as predicted from Alphafold. For this reason, a smaller fragment of *tws* cDNA was subcloned into pHis to try to improve recombinant protein expression. The protein solubility calculator, Protein-Sol (Hebditch et al., 2017), predicted the first half (222 amino acids) of TWS was more soluble compared to the other half of the protein (predicted scaled solubility: 0.663 vs. 0.506). Despite the more favorable solubility score, this smaller construct, pHis-TWS(1-222aa), failed to express to detectable level (Figure 2.9).

I then attempted to improve the solubility of recombinant TWS(1-222aa) protein with the addition of a NUS-A tag at the N-terminus (Mishra, 2020). This approach successfully improved the solubility of this recombinant pHisNUSA-TWS(1-222aa) protein (Figure 2.10A). Due to the expression of soluble protein, pHisNUSA-TWS(1-222aa) was purified using an automated affinity chromatography system (NGC chromatography system, BioRad) (Figure 2.10B). Because the NUS-A tag is much larger than the TWS(1-222aa) fragment (59 kD vs. 25 kD) and can interfere with producing an effective α-TWS antibody, the NUS-A tag needed to be cleaved off the recombinant TWS(1-222aa) protein prior to immunization into animals. The tag was cleaved using TEV protease and separated from TWS(1-222aa). Because the NUS-A tag and

TEV protease both have 6xHis tags, they both bind to the IMAC column during sample application, and the TWS(1-222aa) protein would flow-through the column to be collected (Figure 2.10C). However, SDS-PAGE gel electrophoresis showed that little to no TWS(1-222aa) was collected. All these attempts culminated to my decision to choosing a different portion of TWS to use as an antigen for producing a TWS polyclonal antibody.

The protein structure prediction program, AlphaFold, allowed me to choose a globular region of TWS to increase the likelihood the recombinant protein I generate is soluble (Shen, 2019). However, the resulting recombinant pHis-TWS(231-392aa) antigen was insoluble, which makes it more difficult (but not impossible) to produce an effective antibody. Because the insoluble pHis-TWS(231-392aa) would clog the automated affinity chromatography system, the use of a gravity column allowed us to manually purify pHis-TWS(231-392aa) for antibody production. In *Drosophila* S2 cells, I observed one antibody (7279) exhibited more signal and less background noise after multiple immunizations of the antigen; however, the other antibody (7280) showed non-specific binding (Figure 2.4). When validating the antibodies in *GFP-FLAG-TWS* flies, both antibodies were able to detect TWS with varying success. For #7279, there was lower non-specific binding, but there was little difference in signal when detecting for TWS (Figure 2.5A). However, I observed that there was an increased signal when detecting for TWS in #7280 (Figure 2.5B). To see how the antibody performs in wild type flies, I tested antibody #7279 in wild type samples entrained in summer or winter conditions and found that TWS was most likely to be detected in the two bands around the 50 kD marker in each sample. To further support the utility of this antibody, I would need to demonstrate more directly that these are the correct bands by manipulating *tws* gene expression through RNAi (knock down) or

overexpression. Because there does not seem to be a difference in signal after multiple immunizations, it is possible that TWS(231-392aa) does not produce a sufficient immune response. If this is the case, then there is another recombinant insoluble protein, pHis-TWS(61-222aa), available to produce a TWS polyclonal antibody that may exhibit a higher immune response (Figure 2.2A).

Conclusion

In summary, this study began to explore the possible molecular mechanism of the role of EYA in promoting reproductive dormancy through the physical interaction between EYA and TWS. In previously published results, EYA protein expression cycles over the 24 hours with peak protein expression shifting from day to nighttime in laboratory simulated summer and winter conditions respectively (Abrieux et al., 2020). However, when I measured summer and winter EYA protein expression in the fly strain expressing GFP-TWS as a fusion tag, EYA expression was not cycling in either condition, which was inconsistent with EYA expression measured in a wildtype strain in this study and our previously published findings. The GFP fusion tag is suspected to have contributed to the inconsistency in EYA expression patterns between these two fly strains.

Because large fusion tags can alter protein function, I produced a polyclonal antibody to detect TWS in wildtype flies, which has so far been able to successfully detect TWS in *Drosophila* S2 cells and the fly strain, *GFP-FLAG-TWS*. Further validation via knockdown (RNAi) and/or overexpression of TWS is required to confirm the polyclonal antibody can detect TWS in wildtype flies. This antibody will allow future experiments to better understand the potential role of TWS in reproductive dormancy and seasonal biology in *Drosophila melanogaster*. Many experiments cannot be performed without a functional antibody that can detect endogenous levels of proteins. These might include coimmunoprecipitation experiments to assay how interaction between TWS and EYA in fly tissues might change with seasons and immunostaining to detect cellular and subcellular localization of TWS and how that might be altered in different

seasonal conditions. Results from these experiments will provide insights into the role of TWS seasonal biology.

References

Abrieux, A., Xue, Y., Cai, Y., Lewald, K. M., Nguyen, H. N., Zhang, Y., & Chiu, J. C. (2020). EYES ABSENT and TIMELESS integrate photoperiodic and temperature cues to regulate seasonal physiology in Drosophila. *Proceedings of the National Academy of Sciences*, *117*(26), 15293–15304. https://doi.org/10.1073/pnas.2004262117

Akaba, Y., Takeguchi, R., Tanaka, R., & Takahashi, S. (2021). A Complex Phenotype of a Patient with Spastic Paraplegia Type 4 Caused by a Novel Pathogenic Variant in the SPAST Gene. *Case Reports in Neurology*, *13*(3), 763–771. https://doi.org/10.1159/000520433

Alberts, B., Johnson, A., Lewis, J., Raff, M., Roberts, K., & Walter, P. (2002). B Cells and Antibodies. *Molecular Biology of the Cell. 4th Edition*. https://www.ncbi.nlm.nih.gov/books/NBK26884/

Anduaga, A. M., Nagy, D., Costa, R., & Kyriacou, C. P. (2018). Diapause in Drosophila melanogaster – Photoperiodicity, cold tolerance and metabolites. *Journal of Insect Physiology*, *105*, 46–53. https://doi.org/10.1016/j.jinsphys.2018.01.003

Bolander, M. E., Robey, P. G., Fisher, L. W., Conn, K. M., Prabhakar, B. S., & Termine, J. D. (1989). Monoclonal antibodies against osteonectin show conservation of epitopes across species. *Calcified Tissue International*, *45*(2), 74–80. https://doi.org/10.1007/BF02561405

Bonini, N. M., Leiserson, W. M., & Benzer, S. (1993). The eyes absent gene: Genetic control of cell survival and differentiation in the developing Drosophila eye. *Cell*, *72*(3), 379–395. https://doi.org/10.1016/0092-8674(93)90115-7

Borisov, S. N., Iakovlev, I. K., Borisov, A. S., Ganin, M. Yu., & Tiunov, A. V. (2020). Seasonal Migrations of Pantala flavescens (Odonata: Libellulidae) in Middle Asia and Understanding of the Migration Model in the Afro-Asian Region Using Stable Isotopes of Hydrogen. *Insects*, *11*(12), 890. https://doi.org/10.3390/insects11120890

Bradbury, A. R. M., Trinklein, N. D., Thie, H., Wilkinson, I. C., Tandon, A. K., Anderson, S., Bladen, C. L., Jones, B., Aldred, S. F., Bestagno, M., Burrone, O., Maynard, J., Ferrara, F., Trimmer, J. S., Görnemann, J., Glanville, J., Wolf, P., Frenzel, A., Wong, J., … Dübel, S. (2018). When monoclonal antibodies are not monospecific: Hybridomas frequently express additional functional variable regions. *MAbs*, *10*(4), 539–546. https://doi.org/10.1080/19420862.2018.1445456

Bradshaw, W. E., & Phillips, D. L. (1979). Photoperiodism and the photic environment of the pitcher-plant mosquito, Wyeomyia smithii. *Oecologia*, *44*(3), 311–316. https://doi.org/10.1007/BF00545233

Chmura, H. E., Duncan, C., Saer, B., Moore, J. T., Barnes, B. M., Loren Buck, C., Christian, H. C., Loudon, A. S. I., & Williams, C. T. (2022). Hypothalamic remodeling of thyroid hormone signaling during hibernation in the arctic ground squirrel. *Communications Biology*, *5*(1), 1–13. https://doi.org/10.1038/s42003-022-03431-8

Costantini, L. M., & Snapp, E. L. (2015). Going Viral with Fluorescent Proteins. *Journal of Virology*, *89*(19), 9706–9708. https://doi.org/10.1128/JVI.03489-13

Dawson, A., King, V. M., Bentley, G. E., & Ball, G. F. (2001). Photoperiodic Control of Seasonality in Birds. *Journal of Biological Rhythms*, *16*(4), 365–380. https://doi.org/10.1177/074873001129002079

Denlinger, D. L. (Ed.). (2022). Molecular Signaling Pathways that Regulate Diapause. In *Insect Diapause* (pp. 240–292). Cambridge University Press. https://doi.org/10.1017/9781108609364.010

Dupré, S. M., Miedzinska, K., Duval, C. V., Yu, L., Goodman, R. L., Lincoln, G. A., Davis, J. R. E., McNeilly, A. S., Burt, D. D., & Loudon, A. S. I. (2010). Identification of Eya3 and TAC1 as Long-Day Signals in the Sheep Pituitary. *Current Biology*, *20*(9), 829–835. https://doi.org/10.1016/j.cub.2010.02.066

Eaglesham, J. B., Garcia, A., & Berkmen, M. (2021). Chapter Five—Production of antibodies in SHuffle Escherichia coli strains. In Z. Kelman & W. B. O'Dell (Eds.), *Methods in Enzymology* (Vol. 659, pp. 105–144). Academic Press. https://doi.org/10.1016/bs.mie.2021.06.040

Ecker, D. M., Jones, S. D., & Levine, H. L. (2015). The therapeutic monoclonal antibody market. *MAbs*, *7*(1), 9–14. https://doi.org/10.4161/19420862.2015.989042

Flockhart, D. T. T., Fitz-gerald, B., Brower, L. P., Derbyshire, R., Altizer, S., Hobson, K. A., Wassenaar, L. I., & Norris, D. R. (2017). Migration distance as a selective episode for wing morphology in a migratory insect. *Movement Ecology*, *5*(1), 7. https://doi.org/10.1186/s40462-017-0098-9

Flockhart, D. T. T., Wassenaar, L. I., Martin, T. G., Hobson, K. A., Wunder, M. B., & Norris, D. R. (2013). Tracking multi-generational colonization of the breeding grounds by monarch butterflies in eastern North America. *Proceedings of the Royal Society B: Biological Sciences*, *280*(1768), 20131087. https://doi.org/10.1098/rspb.2013.1087

Galfrè, G., & Milstein, C. (1981). [1] Preparation of monoclonal antibodies: Strategies and procedures. In *Methods in Enzymology* (Vol. 73, pp. 3–46). Academic Press. https://doi.org/10.1016/0076-6879(81)73054-4

Giordani, G. M., Diniz, F., Fussiger, H., Gonzalez-Salazar, C., Donis, K. C., Freua, F., Ortega, R. P. M., de Freitas, J. L., Barsottini, O. G. P., Rosemberg, S., Kok, F., Pedroso, J. L., França, M. C., & Saute, J. A. M. (2021). Clinical and molecular characterization of a large cohort of childhood onset hereditary spastic paraplegias. *Scientific Reports*, *11*(1), 22248. https://doi.org/10.1038/s41598-021-01635-2

Guide to Using the Multiple Sequence Alignment Viewer. (2022). https://www.ncbi.nlm.nih.gov/tools/msaviewer/tutorial1/

Gwinner, E. (1996). Circadian and circannual programmes in avian migration. *Journal of Experimental Biology*, *199*(1), 39–48. https://doi.org/10.1242/jeb.199.1.39

Hebditch, M., Carballo-Amador, M. A., Charonis, S., Curtis, R., & Warwicker, J. (2017). Protein–Sol: A web tool for predicting protein solubility from sequence. *Bioinformatics*, *33*(19), 3098–3100. https://doi.org/10.1093/bioinformatics/btx345

Heo, M., Nord, A. L., Chamousset, D., van Rijn, E., Beaumont, H. J. E., & Pedaci, F. (2017). Impact of fluorescent protein fusions on the bacterial flagellar motor. *Scientific Reports*, *7*(1), 12583. https://doi.org/10.1038/s41598-017-11241-w

Hong, S. M., & Stetson, M. H. (1986). Functional Maturation of the Gonads of Turkish Hamsters under Various Photoperiods1. *Biology of Reproduction*, *35*(4), 858–862. https://doi.org/10.1095/biolreprod35.4.858

Howard, G. C., & Kaser, M. R. (2013). *Making and Using Antibodies: A Practical Handbook, Second Edition*. CRC Press.

Huang, W.-Y., Aramburu, J., Douglas, P. S., & Izumo, S. (2000). Transgenic expression of green fluorescence protein can cause dilated cardiomyopathy. *Nature Medicine*, *6*(5), 482–483. https://doi.org/10.1038/74914

Jumper, J., Evans, R., Pritzel, A., Green, T., Figurnov, M., Ronneberger, O., Tunyasuvunakool, K., Bates, R., Žídek, A., Potapenko, A., Bridgland, A., Meyer, C., Kohl, S. A. A., Ballard, A. J., Cowie, A., Romera-Paredes, B., Nikolov, S., Jain, R., Adler, J., … Hassabis, D. (2021). Highly accurate protein structure prediction with AlphaFold. *Nature*, *596*(7873), 583–589. https://doi.org/10.1038/s41586-021-03819-2

Kaplon, H., Chenoweth, A., Crescioli, S., & Reichert, J. M. (2022). Antibodies to watch in 2022. *MAbs*, *14*(1), 2014296. https://doi.org/10.1080/19420862.2021.2014296

Kennedy, P. J., Oliveira, C., Granja, P. L., & Sarmento, B. (2018). Monoclonal antibodies: Technologies for early discovery and engineering. *Critical Reviews in Biotechnology*, *38*(3), 394–408. https://doi.org/10.1080/07388551.2017.1357002

Koerber, J. T., Jang, J.-H., Yu, J. H., Kane, R. S., & Schaffer, D. V. (2007). Engineering Adeno-Associated Virus for One-Step Purification via Immobilized Metal Affinity Chromatography. *Human Gene Therapy*, *18*(4), 367–378. https://doi.org/10.1089/hum.2006.139

Köhler, G., & Milstein, C. (1975). Continuous cultures of fused cells secreting antibody of predefined specificity. *Nature*, *256*(5517), 495–497. https://doi.org/10.1038/256495a0

Kuo, Y.-W., Trottier, O., Mahamdeh, M., & Howard, J. (2019). Spastin is a dual-function enzyme that severs microtubules and promotes their regrowth to increase the number and mass of microtubules. *Proceedings of the National Academy of Sciences*, *116*(12), 5533–5541. https://doi.org/10.1073/pnas.1818824116

Larouche, M., Kachaner, D., Wang, P., Normandin, K., Garrido, D., Yao, C., Cormier, M., Johansen, K. M., Johansen, J., & Archambault, V. (2021). Spatiotemporal coordination of Greatwall-Endos-PP2A promotes mitotic progression. *Journal of Cell Biology*, *220*(6), e202008145. https://doi.org/10.1083/jcb.202008145

Legan, S. J., & Winans, S. S. (1981). The photoneuroendocrine control of seasonal breeding in the ewe. *General and Comparative Endocrinology*, *45*(3), 317–328. https://doi.org/10.1016/0016-6480(81)90072-1

Lipman, N. S., Jackson, L. R., Trudel, L. J., & Weis-Garcia, F. (2005). Monoclonal Versus Polyclonal Antibodies: Distinguishing Characteristics, Applications, and Information Resources. *ILAR Journal*, *46*(3), 258–268. https://doi.org/10.1093/ilar.46.3.258

Margolin, W. (2012). The Price of Tags in Protein Localization Studies. *Journal of Bacteriology*, *194*(23), 6369–6371. https://doi.org/10.1128/JB.01640-12

Mayer-Jaekel, R. E., Ohkura, H., Ferrigno, P., Andjelkovic, N., Shiomi, K., Uemura, T., Glover, D. M., & Hemmings, B. A. (1994). Drosophila mutants in the 55 kDa regulatory subunit of protein phosphatase 2A show strongly reduced ability to dephosphorylate substrates of p34cdc2. *Journal of Cell Science*, *107*(9), 2609–2616. https://doi.org/10.1242/jcs.107.9.2609

McGraw, J., Tatipelli, V. K., Feyijinmi, O., Traore, M. C., Eangoor, P., Lane, S., & Stollar, E. J. (2014). A semi-automated method for purification of milligram quantities of proteins on the QIAcube. *Protein Expression and Purification*, *96*, 48–53. https://doi.org/10.1016/j.pep.2014.01.014

Merlin, C., Iiams, S. E., & Lugena, A. B. (2020). Monarch Butterfly Migration Moving into the Genetic Era. *Trends in Genetics*, *36*(9), 689–701. https://doi.org/10.1016/j.tig.2020.06.011

Mishra, V. (2020). Affinity Tags for Protein Purification. *Current Protein & Peptide Science*, *21*(8), 821–830.

Morimoto, Y. V., Namba, K., & Minamino, T. (2020). GFP Fusion to the N-Terminus of MotB Affects the Proton Channel Activity of the Bacterial Flagellar Motor in Salmonella. *Biomolecules*, *10*(9), 1255. https://doi.org/10.3390/biom10091255

Murphy, M., Jethwa, P. H., Warner, A., Barrett, P., Nilaweera, K. N., Brameld, J. M., & Ebling, F. J. P. (2012). Effects of Manipulating Hypothalamic Triiodothyronine Concentrations on Seasonal Body Weight and Torpor Cycles in Siberian Hamsters. *Endocrinology*, *153*(1), 101–112. https://doi.org/10.1210/en.2011-1249

Nagy, D., Andreatta, G., Bastianello, S., Martín Anduaga, A., Mazzotta, G., Kyriacou, C. P., & Costa, R. (2018). A Semi-natural Approach for Studying Seasonal Diapause in Drosophila melanogaster Reveals Robust Photoperiodicity. *Journal of Biological Rhythms*, *33*(2), 117–125. https://doi.org/10.1177/0748730417754116

Nakao, N., Ono, H., Yamamura, T., Anraku, T., Takagi, T., Higashi, K., Yasuo, S., Katou, Y., Kageyama, S., Uno, Y., Kasukawa, T., Iigo, M., Sharp, P. J., Iwasawa, A., Suzuki, Y.,

Sugano, S., Niimi, T., Mizutani, M., Namikawa, T., … Yoshimura, T. (2008). Thyrotrophin in the pars tuberalis triggers photoperiodic response. *Nature*, *452*(7185), 317–322. https://doi.org/10.1038/nature06738

Norris, S. R., Núñez, M. F., & Verhey, K. J. (2015). Influence of Fluorescent Tag on the Motility Properties of Kinesin-1 in Single-Molecule Assays. *Biophysical Journal*, *108*(5), 1133–1143. https://doi.org/10.1016/j.bpj.2015.01.031

Ojima, N., Hara, Y., Ito, H., & Yamamoto, D. (2018). Genetic dissection of stress-induced reproductive arrest in Drosophila melanogaster females. *PLOS Genetics*, *14*(6), e1007434. https://doi.org/10.1371/journal.pgen.1007434

Peltomaa, R., Barderas, R., Benito-Peña, E., & Moreno-Bondi, M. C. (2022). Recombinant antibodies and their use for food immunoanalysis. *Analytical and Bioanalytical Chemistry*, *414*(1), 193–217. https://doi.org/10.1007/s00216-021-03619-7

Reppert, S. M., & de Roode, J. C. (2018). Demystifying Monarch Butterfly Migration. *Current Biology*, *28*(17), R1009–R1022. https://doi.org/10.1016/j.cub.2018.02.067

Ruf, T., & Geiser, F. (2015). Daily torpor and hibernation in birds and mammals. *Biological Reviews*, *90*(3), 891–926. https://doi.org/10.1111/brv.12137

Sathyanarayanan, S., Zheng, X., Xiao, R., & Sehgal, A. (2004). Posttranslational Regulation of Drosophila PERIOD Protein by Protein Phosphatase 2A. *Cell*, *116*(4), 603–615. https://doi.org/10.1016/S0092-8674(04)00128-X

Saunders, D. S., & Gilbert, L. I. (1990). Regulation of ovarian diapause in Drosophila melanogaster by photoperiod and moderately low temperature. *Journal of Insect Physiology*, *36*(3), 195–200. https://doi.org/10.1016/0022-1910(90)90122-V

Seidel, A., Heldmaier, G., & Schulz, F. (1987). Seasonal changes in circulating levels of thyroid hormones are not dependent on the age in djungarian hamsters phodopus sungorus. *Comparative Biochemistry and Physiology Part A: Physiology*, *88*(1), 71–73. https://doi.org/10.1016/0300-9629(87)90101-0

Sharma, A., Tripathi, V., & Kumar, V. (2022). Control and adaptability of seasonal changes in behavior and physiology of latitudinal avian migrants: Insights from laboratory studies in Palearctic-Indian migratory buntings. *Journal of Experimental Zoology Part A: Ecological and Integrative Physiology*, *n/a*(n/a). https://doi.org/10.1002/jez.2631

Shen, C.-H. (2019). Chapter 4 - Gene Expression: Translation of the Genetic Code. In C.-H. Shen (Ed.), *Diagnostic Molecular Biology* (pp. 87–116). Academic Press. https://doi.org/10.1016/B978-0-12-802823-0.00004-3

Sim, C., & Denlinger, D. (2013). Insulin signaling and the regulation of insect diapause. *Frontiers in Physiology*, *4*. https://www.frontiersin.org/articles/10.3389/fphys.2013.00189

Solowska, J. M., D'Rozario, M., Jean, D. C., Davidson, M. W., Marenda, D. R., & Baas, P. W. (2014). Pathogenic Mutation of Spastin Has Gain-of-Function Effects on Microtubule Dynamics. *Journal of Neuroscience*, *34*(5), 1856–1867. https://doi.org/10.1523/JNEUROSCI.3309-13.2014

Swulius, M. T., & Jensen, G. J. (2012). The Helical MreB Cytoskeleton in Escherichia coli MC1000/pLE7 Is an Artifact of the N-Terminal Yellow Fluorescent Protein Tag. *Journal of Bacteriology*, *194*(23), 6382–6386. https://doi.org/10.1128/JB.00505-12

Thaben, P. F., & Westermark, P. O. (2014). Detecting Rhythms in Time Series with RAIN. *Journal of Biological Rhythms*, *29*(6), 391–400. https://doi.org/10.1177/0748730414553029

Varadi, M., Anyango, S., Deshpande, M., Nair, S., Natassia, C., Yordanova, G., Yuan, D., Stroe, O., Wood, G., Laydon, A., Žídek, A., Green, T., Tunyasuvunakool, K., Petersen, S., Jumper, J., Clancy, E., Green, R., Vora, A., Lutfi, M., … Velankar, S. (2022). AlphaFold Protein Structure Database: Massively expanding the structural coverage of protein-sequence space with high-accuracy models. *Nucleic Acids Research*, *50*(D1), D439–D444. https://doi.org/10.1093/nar/gkab1061

Varghaei, P., Estiar, M. A., Ashtiani, S., Veyron, S., Mufti, K., Leveille, E., Yu, E., Spiegelman, D., Rioux, M.-F., Yoon, G., Tarnopolsky, M., Boycott, K. M., Dupre, N., Suchowersky, O., Trempe, J.-F., Rouleau, G. A., & Gan-Or, Z. (2022). Genetic, structural and clinical analysis of spastic paraplegia 4. *Parkinsonism & Related Disorders*, *98*, 62–69. https://doi.org/10.1016/j.parkreldis.2022.03.019

Wang, C., Shui, K., Ma, S., Lin, S., Zhang, Y., Wen, B., Deng, W., Xu, H., Hu, H., Guo, A., Xue, Y., & Zhang, L. (2020). Integrated omics in Drosophila uncover a circadian kinome. *Nature Communications*, *11*(1), 2710. https://doi.org/10.1038/s41467-020-16514-z

Zhang, L., Zhou, H., Li, X., Vartuli, R. L., Rowse, M., Xing, Y., Rudra, P., Ghosh, D., Zhao, R., & Ford, H. L. (2018). Eya3 partners with PP2A to induce c-Myc stabilization and tumor progression. *Nature Communications*, *9*(1), 1047. https://doi.org/10.1038/s41467-018-03327-4

Zou, J., Cai, Z., Liang, Z., Liang, Y., Zhang, G., Yang, J., Zhang, Y., Lin, H., & Tan, M. (2021). Different fusion tags affect the activity of ubiquitin overexpression on spastin protein stability. *European Journal of Histochemistry*, *65*(4), Article 4. https://doi.org/10.4081/ejh.2021.3352

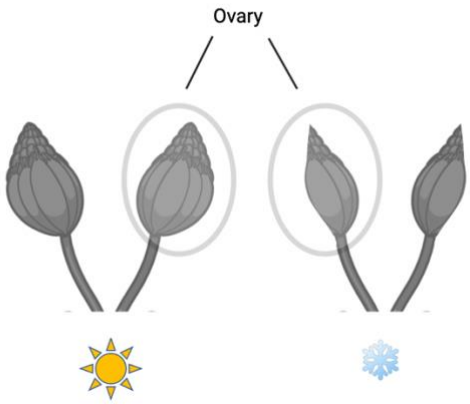

Figure 1.1 Ovary size varies depending on the season where they are larger in the summer (left) and smaller in the winter (right) (Abrieux et al., 2020).

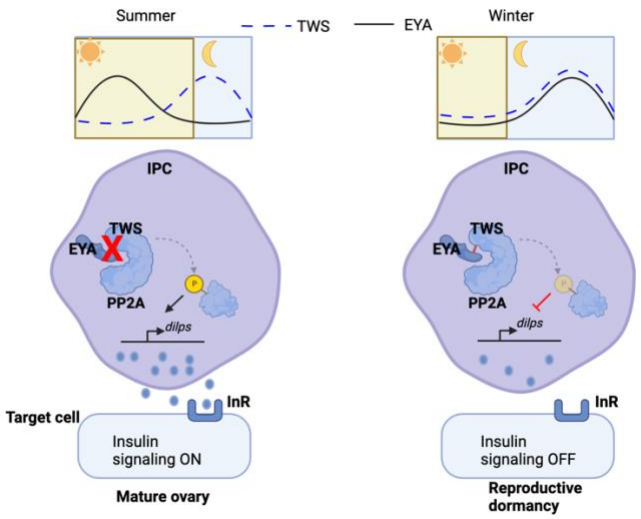

Figure 1.2 Proposed coincidence model for the role of EYA in seasonal reproductive dormancy (Chiu, unpublished). Because EYA expression peaks during the evening only in the winter (Abrieux et al., 2020), TWS and EYA expression only correspond during this time. In the summer, EYA peak expression is during the day, while TWS peak expression is at night. Due to lower EYA protein expression at night, there is a lower probability that EYA will bind to the TWS subunit, which leaves PP2A inactive and the insulin signaling pathway activated, resulting in mature ovaries. In the winter, EYA and TWS both have peak expression during the night, so it is more likely they will interact and activate the role of EYA as a regulator of PP2A. This activation allows PP2A to dephosphorylate key proteins in the insulin signaling pathway, which inhibits insulin signaling and induces reproductive dormancy.

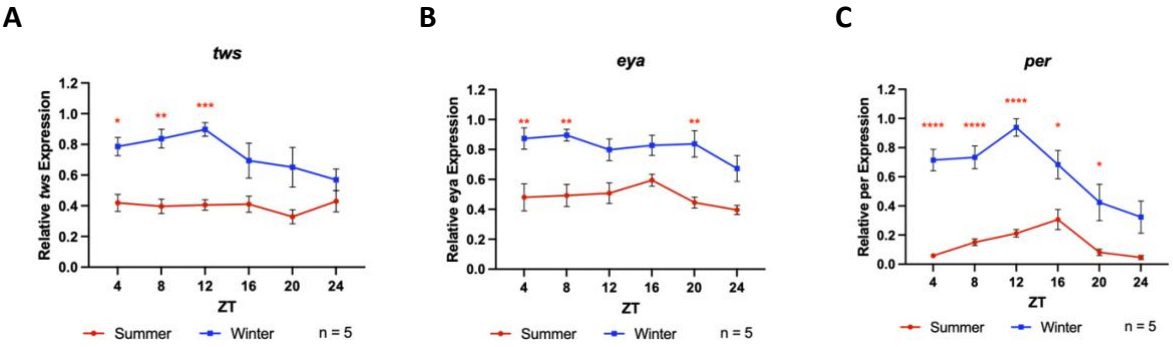

Figure 1.3 *tws*, *eya*, and *per* mRNA expression in summer and winter conditions. Comparison of mRNA expression between *tws*, *eya*, and *per* normalized to non-cycling *cbp20*. A) *tws* has rhythmic mRNA expression in winter (p-value = 0.034; peak = ZT12; RAIN), but not in summer conditions (p-value = 0.85; RAIN). B) *eya* has rhythmic mRNA expression in summer (p-value = 0.041; peak = ZT16; RAIN), but not in winter conditions (p-value = 0.94; RAIN). C) *per* is a known cycling gene and the positive control. It has rhythmic mRNA expression in both summer (p-value = 1.60E-08; peak = ZT16; RAIN) and winter conditions (p-value = 2.64E-05; peak = ZT12; RAIN). ZT = Zeitgeber time. Data represented are mean ± SEM of n = 5 biological replicates with two technical replicates each. Summer conditions: 16:8 LD at 25˚C. Winter conditions: 8:16 LD at 10˚C. p-value = * : <0.05; ** : <0.01; ***: <0.001; ****: <0.0001 (Two-way ANOVA with Tukey's multiple comparisons test)

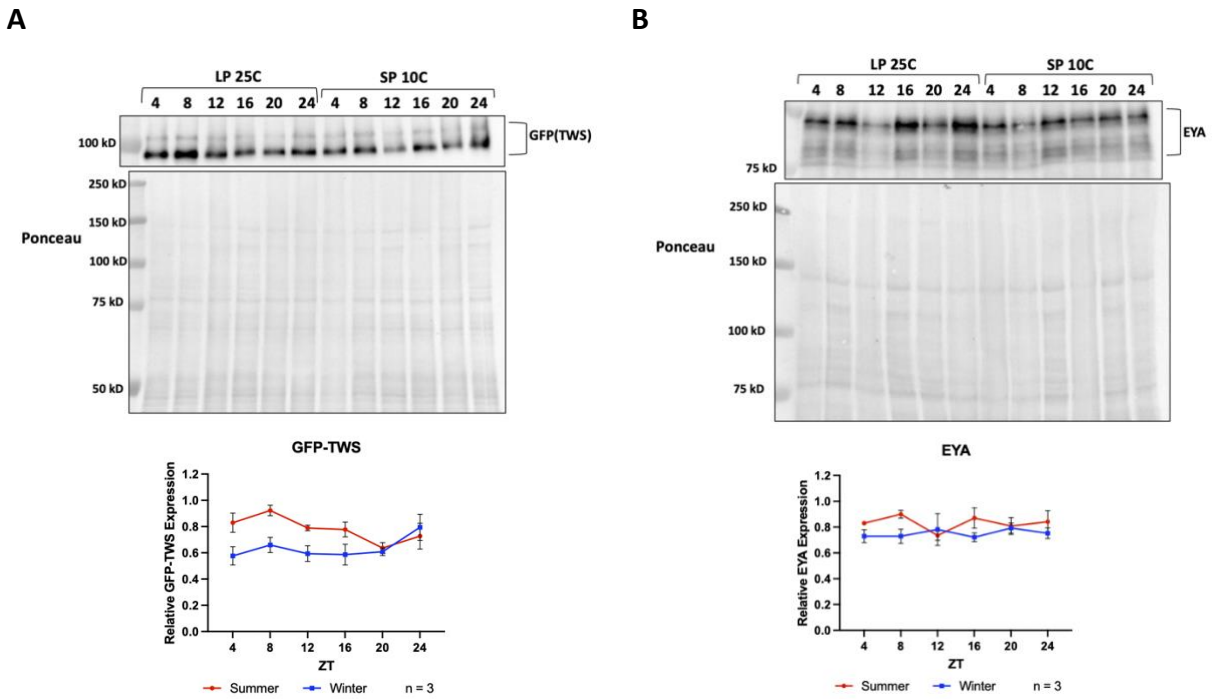

Figure 1.4 GFP-tagged TWS protein expression is rhythmic in summer conditions, but EYA protein expression is not rhythmic in either summer or winter conditions. *GFP-FLAG-TWS* flies were entrained for three days in summer or winter conditions and samples were collected every 4 hours on the 4th day. A) Because TWS was tagged with GFP, TWS protein expression was measured indirectly using the primary antibody, α-GFP, diluted to 1:10,000 and α-rabbit IgG as the secondary antibody. Ponceau (lower panel) stains all proteins and serves as loading control and for normalization. GFP-TWS has rhythmic protein expression in summer (p-value: 0.00038; Peak: ZT 8; RAIN), but not in winter conditions (p-value: 0.29, RAIN). B) EYA protein expression was measured using α-EYA diluted to 1:1000 as the primary antibody and α-mouse diluted to 1:1000 as the secondary antibody. Data represented are mean $\pm$ SEM of n = 3 biological replicates each. Summer conditions: 16:8 LD at 25˚C. Winter conditions: 8:16 LD at 10˚C. p-value = * : <0.05; ** : <0.01; ***: <0.001; ****: <0.0001 (Two-way ANOVA with Tukey test)

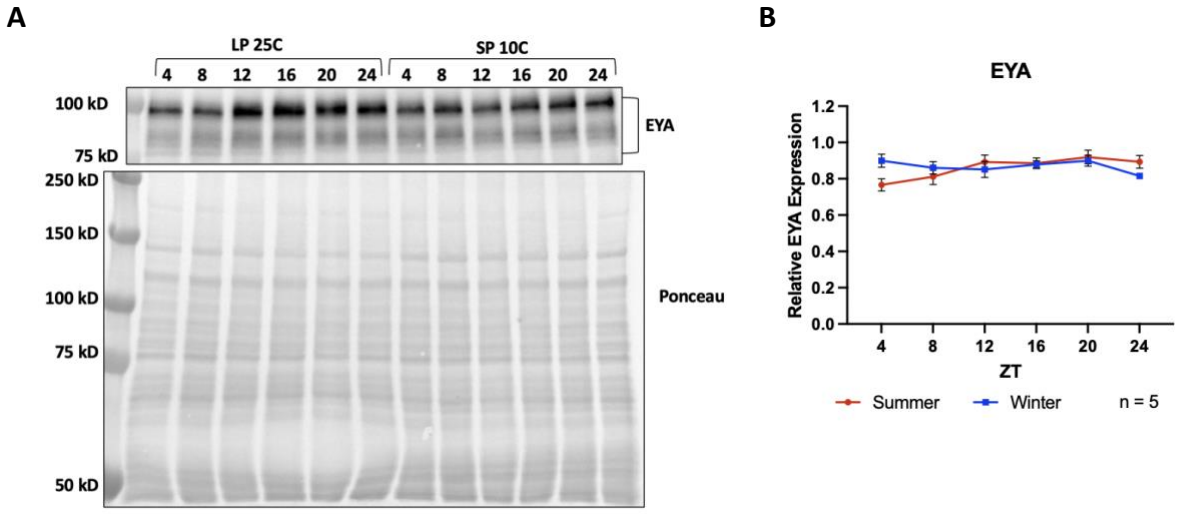

Figure 1.5 EYA protein expression is rhythmic in summer conditions and peaks at ZT 20. Wildtype w^{1118} flies were entrained in 12:12 LD at 25˚C for three days and then moved to summer or winter conditions for seven days. Flies were collected every four hours over a 24-hour period on the seventh day. A) Top: Representative sample showing western blot analysis of EYA protein expression was measured using α-EYA diluted to 1:1000 as the primary antibody and α-mouse diluted to 1:1000 as the secondary antibody. Bottom: Ponceau S staining of top blot, used for loading control and normalization. B) Quantification of EYA protein expression using Ponceau S total protein staining for normalization. EYA has rhythmic protein expression in summer conditions (p-value: = 0.019; Peak: ZT20; RAIN), but not in winter conditions (p-value: 0.72; RAIN). Data represented are mean $\pm$ SEM of n = 5 biological replicates each. Summer conditions: 16:8 LD at 25˚C. Winter conditions: 8:16 LD at 10˚C. p-value = * : <0.05; ** : <0.01; ***: <0.001; ****: <0.0001 (Two-way ANOVA with Tukey test).

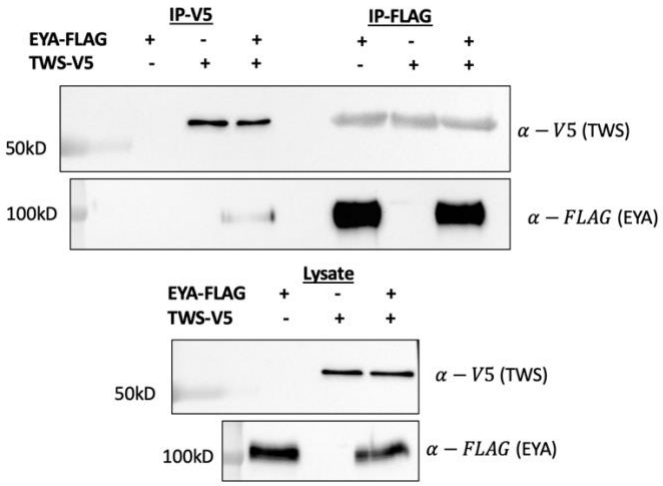

Figure 1.6 EYA and TWS physically interact in *Drosophila* S2 cells. Western blots displaying the results of co-immunoprecipitation (coIP) of EYA and TWS in S2 cells. S2 cell protein extracts were either immunoprecipitated with α-FLAG to detect EYA or with α-V5 to detect TWS. The resulting protein complexes were visualized via Western blot to detect EYA, TWS and EYA-TWS interactions. Lysate is the input for the coIP.

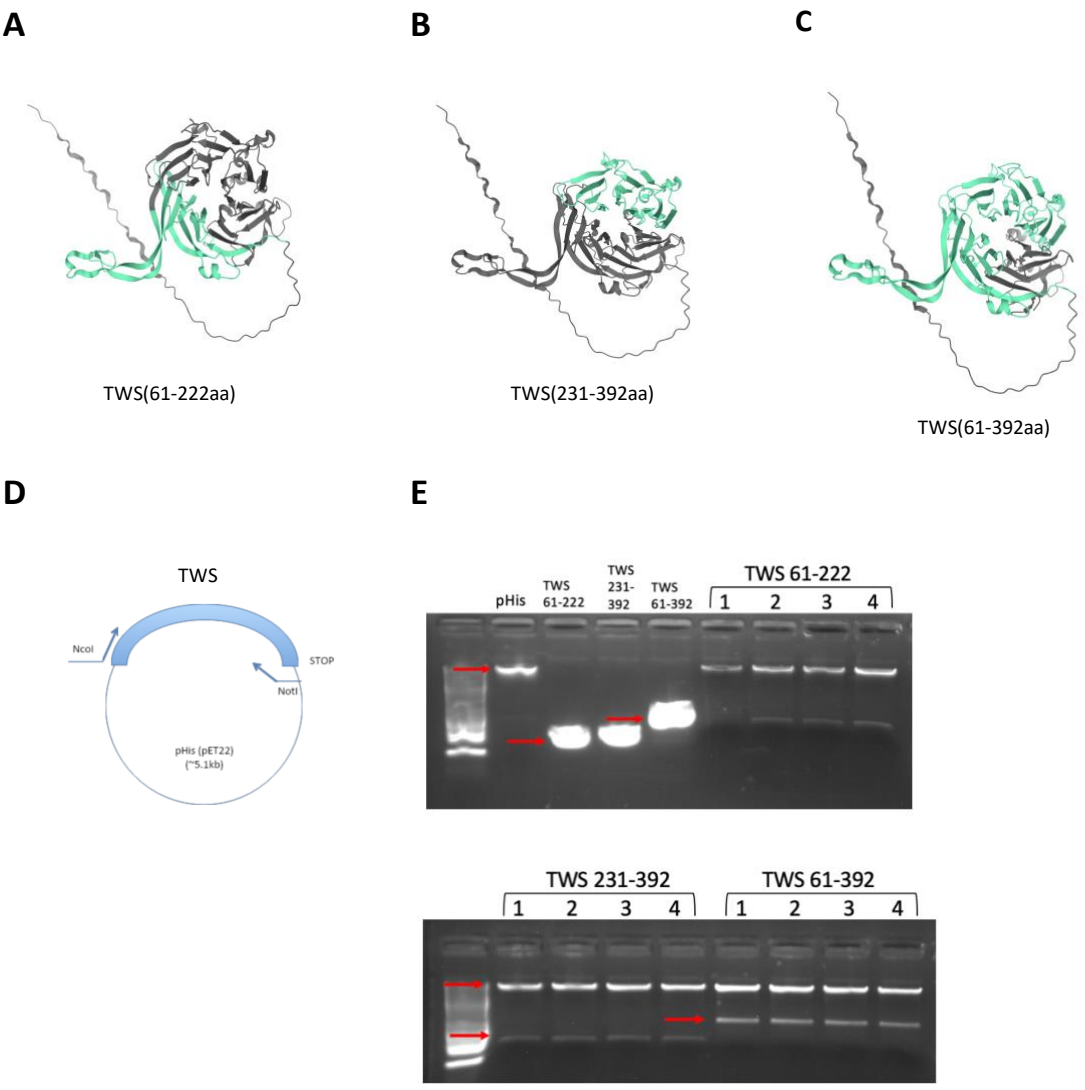

Figure 2.1 AlphaFold protein structure prediction of A) TWS(61-222aa) B) TWS(231-392aa) and C) TWS(61-392aa). Green: portion of TWS subcloned into the pHis expression vector. Black: portion of TWS not subcloned into pHis. D) General model of the pHis-TWS construct design. Each portion of TWS included a STOP codon and was inserted into the pHis expression vector between the NcoI and NotI restriction sites. E) To confirm each portion of TWS was correctly inserted into pHis, 4 colonies from the transformation into DH5α were digested with NotI and NcoI and the products were visualized on an agarose gel. pHis: digested pHis expression vector; TWS 61-222: digested TWS 61-222 PCR product (insert, 483 bp); TWS 231-392: digested TWS 231-392 PCR product (insert, 483 bp); TWS 61-392: digested TWS 61-392 PCR product (insert, 1 kb).

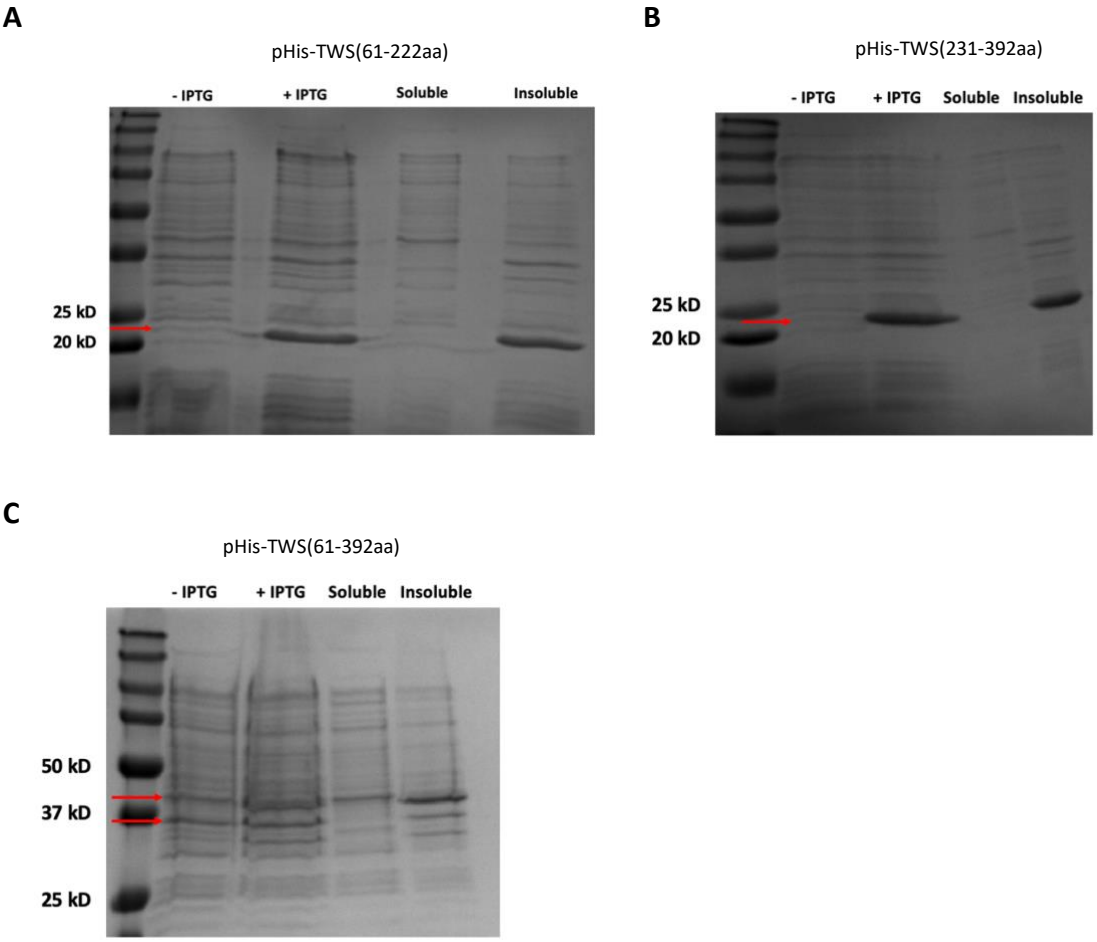

Figure 2.2 SDS-PAGE gels with Coomassie stain to test expression and solubility of A) pHis-TWS(61-222aa), B) pHis-TWS(231-392aa) and C) pHis-TWS(61-392aa). -IPTG: negative control without IPTG induction; +IPTG: IPTG induction; Soluble: supernatant; Insoluble: pellet

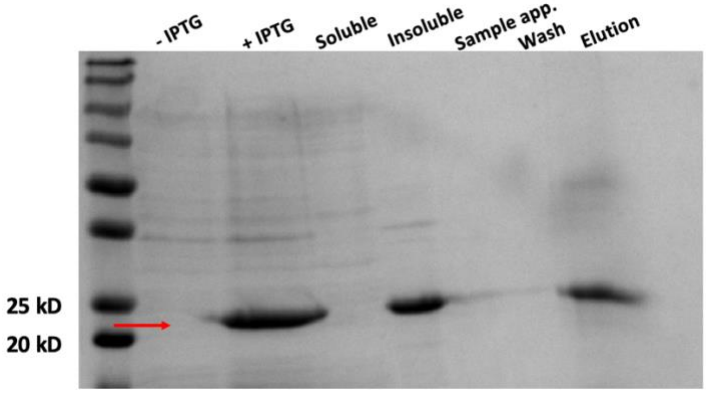

Figure 2.3 Purification of pHis-TWS(231-392aa) visualized via SDS-PAGE gel with Coomassie stain.
-IPTG: negative control without IPTG induction; +IPTG: IPTG induction of pHis-TWS(231-392aa); Soluble: supernatant; Insoluble: pellet; Sample app.: flow-through during the sample application step of protein purification; Wash: flow-through during the wash step of protein purification; Elution: eluted pHis-TWS(231-392aa)

	Volume	Concentration	Total
Before Concentration	~19 mL	674.9 ug/mL	12.823 mg
After Concentration	~5.5 mL	1203.5 ug/mL	6.619 mg
After Dialysis	~5.5 mL	1106.5 ug/mL	6.086 mg

Table 1. Quantification of pHis-TWS(231-392aa) after purification

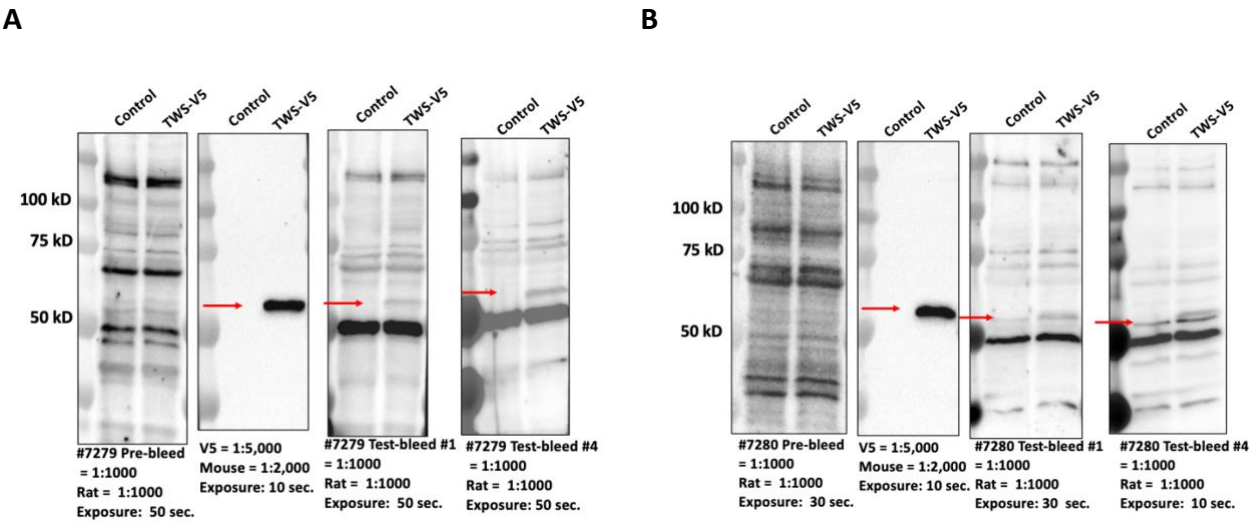

Figure 2.4 Validation of α-TWS antibody in *Drosophila* S2 cells and visualize via western blot. Pre-bleed: negative control (1:1000 dilution); α-V5: positive control (1:5000 dilution); Test-bleed #1 and #4: experimental sample (1:1000 dilution). Control: untransfected S2 cells. TWS-V5: S2 cells transfected with pAc-tws-V5. pHis-TWS(231-392aa) was injected into two rats, A) #7279 and B) #7280

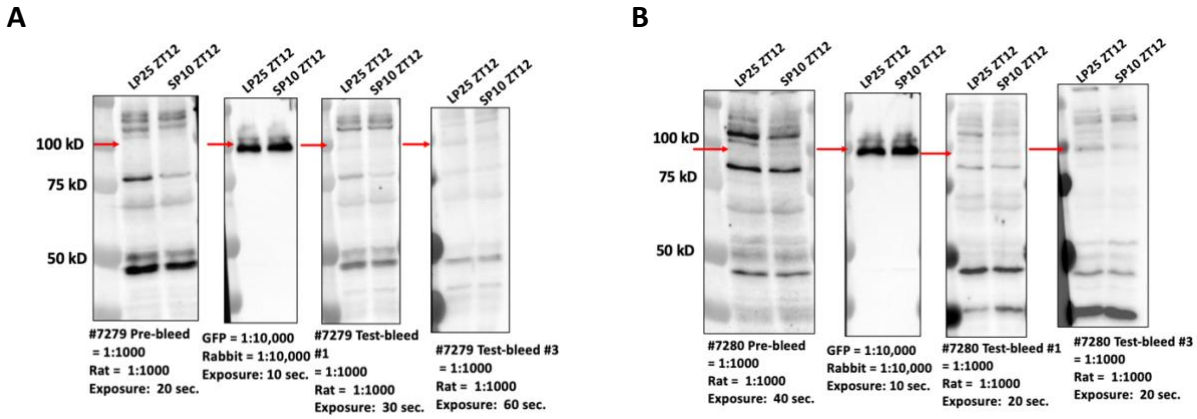

Figure 2.5 Validation of α-TWS antibody in *GFP-FLAG-TWS* fly strain and visualization via Western blot. pHis-TWS(231-392aa) was injected into two rats, A) #7279 and B) #7280. Pre-bleed: negative control (1:1000 dilution); α-GFP: positive control (1:10,000 dilution); Test-bleed #1 and #3: experimental sample (1:1000 dilution). LP25 ZT12: Flies entrained in long photoperiod at 25°C and collected at ZT12. SP10 ZT12: Flies entrained in short photoperiod at 10°C and collected at ZT12. Red arrows indicate the band corresponding to GFP-tagged TWS.

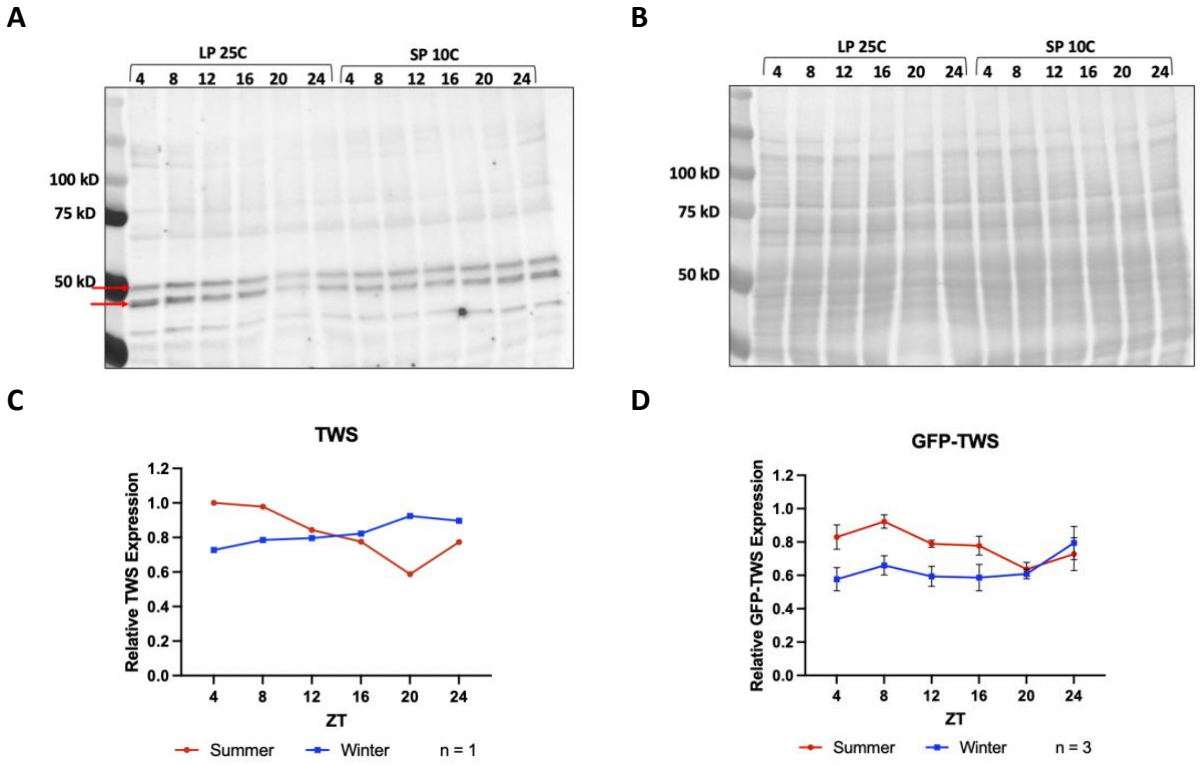

Figure 2.6 Determine TWS protein expression in summer and winter conditions in wildtype *Drosophila*. A) w^{1118} flies were entrained in either long photoperiod conditions at 25°C (summer) or short photoperiod conditions at 10°C (winter) and collected every 4 hours. Using western blot, TWS protein expression was detected using test bleed #4 (#7279) as the primary antibody at dilution 1:1000 and α-rat as the secondary antibody at dilution 1:1000. The red arrows indicate the bands most likely to correspond to TWS expression. B) Ponceau stain measuring total protein expression of the blot from A), which was used for normalization. C) Normalized TWS expression in summer and winter conditions. D) Normalized GFP-tagged TWS expression in summer and winter conditions in *GFP-FLAG-TWS* flies.

A

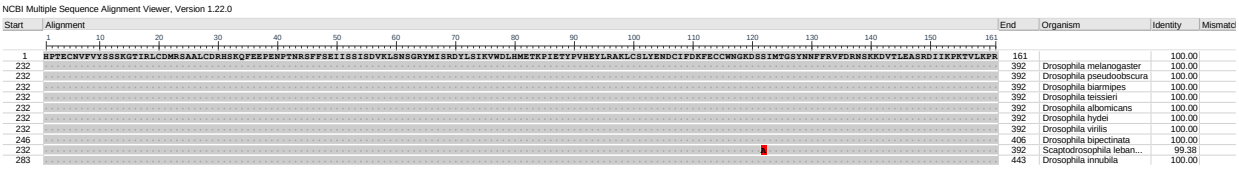

B

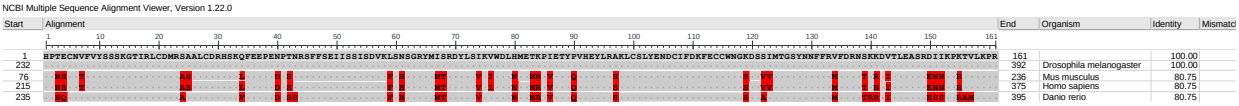

Figure 2.7 Multiple sequence alignment shows conservation between the *Drosophila melanogaster* TWS antigen with TWS protein sequence in A) other *Drosophila* species and B) vertebrate model organisms. Top row: TWS antigen sequence used to produce polyclonal antibody. Start: start of sequence alignment; End: end of sequence alignment; Organism: species; Identity: number of matches in an alignment row relative to the alignment length (*Guide to Using the Multiple Sequence Alignment Viewer*, 2022). Mismatches: number of mismatches in the alignment. Gray dots: alignment match. Amino acids highlighted in red: mismatch.

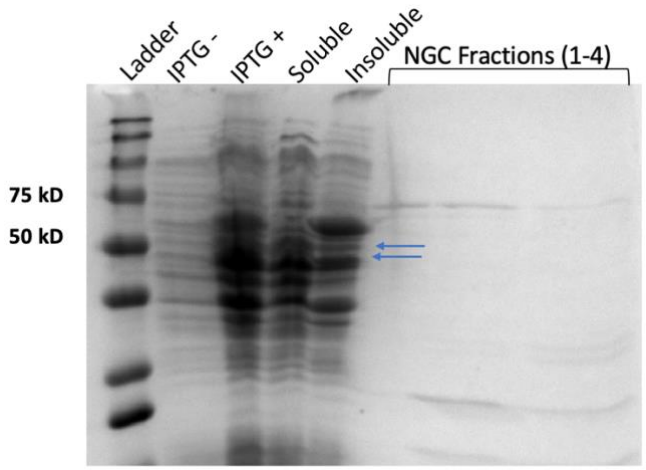

Figure 2.8 Purification of pHis-TWS using the full-length *tws* ORF. Ladder: size markers; IPTG - : pHis-TWS BL21 culture before IPTG induction; IPTG + : pHis-TWS BL21 culture after IPTG induction; Soluble: pHis-TWS BL21 culture supernatant; Insoluble: pHis-TWS BL21 culture pellet; NGC Fractions (1-4): Elution fractions during protein purification. Blue arrows point at possible bands that could contain pHis-TWS (~50kD)

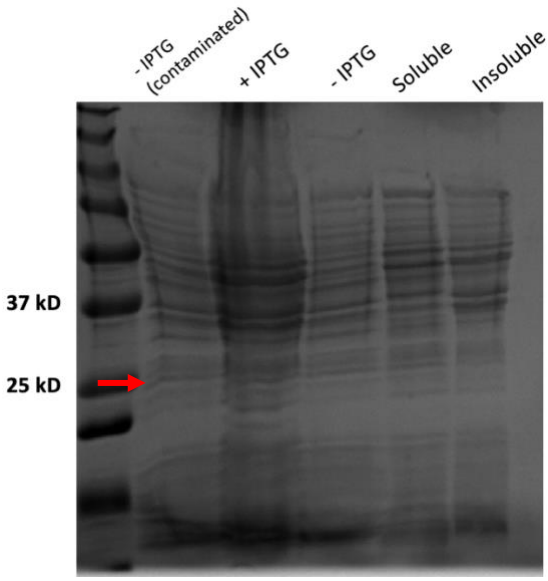

Figure 2.9 pHis-TWS(1-222aa) not expressed (~25kD). IPTG - : pHis-TWS(1-222aa) BL21 culture before IPTG induction; IPTG + : pHis-TWS(1-222aa) BL21 culture after IPTG induction; Soluble: pHis-TWS(1-222aa) BL21 culture supernatant; Insoluble: pHis-TWS(1-222aa) BL21 culture pellet; Red arrow point at possible bands that could contain pHis-TWS(1-222aa) (~25kD).

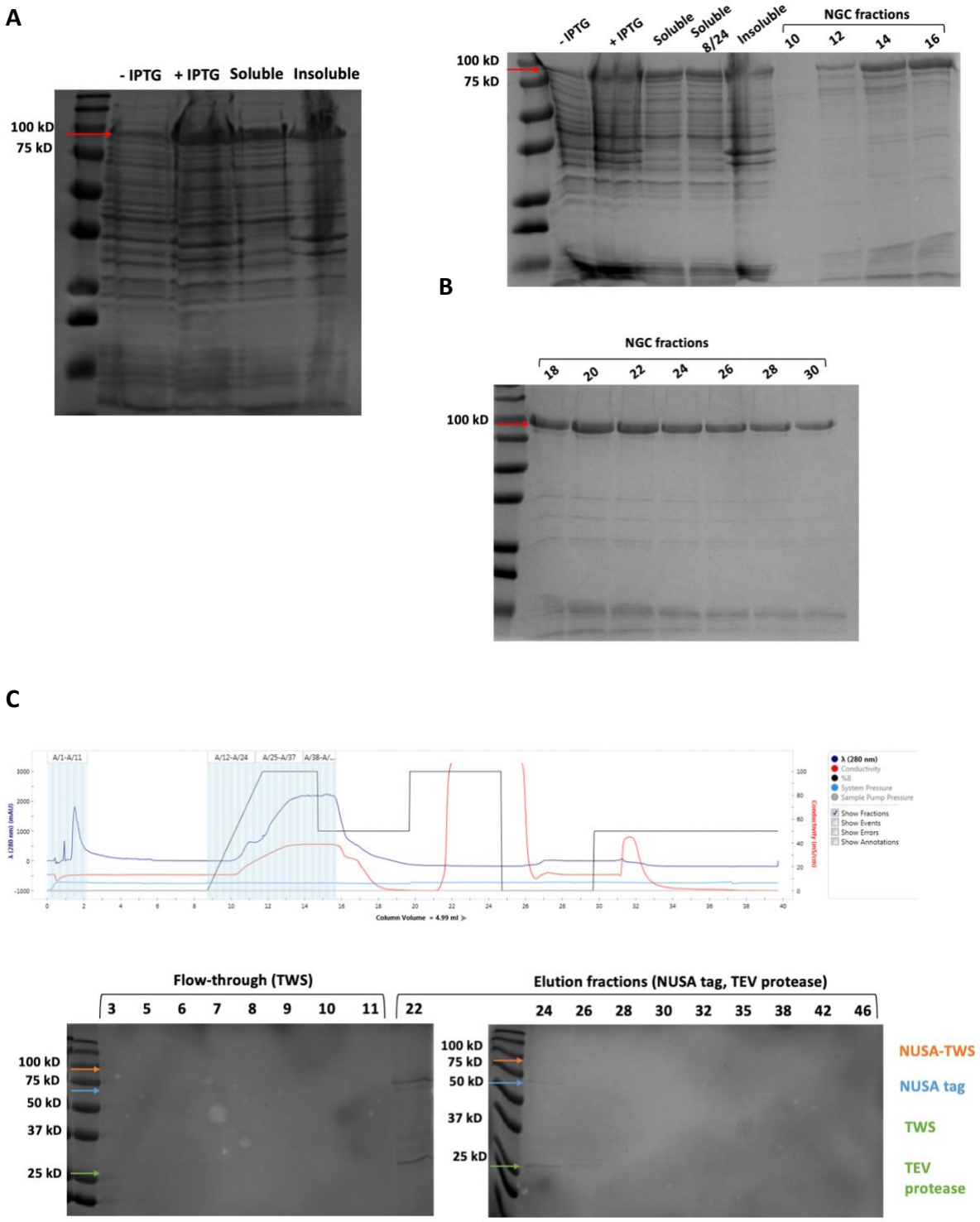

Figure 2.10 pHisNUSA-TWS(1-222aa) expressed and soluble, but not able to recover protein after cleavage of NUSA tag. A) pHisNUSA-TWS(1-222aa) was found to be expressed and soluble when grown in *E. coli* BL21 cell culture. IPTG - : pHisNUSA-TWS(1-222aa) BL21 culture before IPTG induction; IPTG + : pHisNUSA-TWS(1-222aa) BL21 culture after IPTG induction; Soluble: pHisNUSA-TWS(1-222aa) BL21 culture supernatant; Insoluble: pHisNUSA-TWS(1-222aa) BL21 culture pellet; B) After the cell lysis supernatant of pHisNUSA-TWS(1-222aa) was collected and filtered, pHisNUSA-TWS(1-222aa) was separated from the rest of the proteins in the lysate using

an immobilized metal affinity chromatography (IMAC) column on the BioRad NGC chromatography system. Elution fractions #10-30 were collected and visualized on SDS-PAGE gel electrophoresis. Soluble 8/24: thawed pHisNUSA-TWS(1-222aa) BL21 culture supernatant after storage in -80°C. C) The pHisNUSA tag was cleaved using TEV protease and separated from TWS(1-222aa) using an IMAC column on the BioRad NGC chromatography system. Because the tag and the TEV protease include 6XHis, they both should bind to the column, as seen in fractions A22-46 (top, 280 nm line in dark blue). The TWS(1-222aa) no longer has 6XHis, so it should flow through the column during the sample application step as seen in fractions A3-11 (top, 280 nm line in dark blue). Fractions A3-11 and A22-46 were visualized via SDS-PAGE. NUSA-TWS = 84 kD, orange arrow; NUSA tag = 59 kD, blue arrow; TEV protease and TWS(1-222aa) = 25 kD, green arrow.